Fault-tolerant consensus control of multi-agent systems under actuator/sensor faults and channel noises: a distributed anti-attack strategy

Jing Zhao[a], Chun Liu[a,b], Bin Jiang[c], Ron J. Patton[d]

[a]*School of Mechatronic Engineering and Automation, Shanghai University, Shanghai, 200444, China*
[b]*School of Artificial Intelligence, Shanghai University, Shanghai, 200444, China*
[c]*College of Automation Engineering, Nanjing University of Aeronautics and Astronautics, Nanjing, 210016, China*
[d]*School of Engineering and Computer Science, University of Hull, Hull, HU6 7RX, United Kingdom*

Abstract

This study investigates the distributed fault-tolerant consensus control problem of multi-agent systems subject to simultaneous actuator/sensor faults and channel noises in physical layer and hostile connectivity-mixed attacks in cyber layer. Actuator/sensor faults are remodeled into unified abrupt-type and incipient-type characteristics, and connectivity-mixed attacks are established with connectivity-maintained and connectivity-paralyzed topologies by a switching and nonoverlapping version. Normalization and estimation-based observer is devised to recollect unknown state and fault observations, and distributed anti-attack fault-tolerant consensus control is also developed to achieve the tolerance to faults, resilience to attacks and robustness to noises, respectively, with the novel incorporated sensor fault and output channel noise estimation as well as neighboring output information. Criteria of reaching leader-following consensus of multi-agent systems under cyber-physical threats are derived with attack frequency and activation rate technique. Effectiveness and improvements of the proposed fault-tolerant consensus algorithm are validated on two case studies: 1) multi-machine power system synchronization and 2) multi-aircraft system coordination .

Keywords: Fault-tolerant consensus control, distributed anti-attack, multi-agent systems, actuator and sensor faults, connectivity-mixed attacks, channel noises

1. Introduction

Fault-tolerant consensus control of multi-agent systems (MASs) [1] with capabilities of maintaining local and global expected performance when confronted with faults has received a tremendous surge of interest in a wide range of civil-military applications in islanded microgrids [2], underwater vehicles [3], self-driving vehicles [4], unmanned aerial vehicles [5], etc. Unlike conventional fault-tolerant consensus for the general linear MASs [6], the nonlinear factors of MASs bring challenges to the realization of quick consensus and accurate robustness, and hence fault-tolerant consensus classification for the fractional-order nonlinear MASs [7], stochastic nonlinear MASs [8] and switched nonlinear MASs [9] has progressed rapidly. A class of the nonlinear MASs in the presence of heterogeneous and switching characteristics as well as actuator faults is considered with fuzzy logic approximation technique to solve the consensus tracking problem [10]. However, not only unintended failures in the physical layer but also hazardous attacks in the cyber layer can propagate dramatically and rapidly to other agents through contaminated information interactions, thus resulting in local performance destruction or global mission degradation of nonlinear MASs. Thus, fault-tolerance consensus with anti-attack resilience on nonlinear MASs remains its ability and sustainability at a normal prescribed level or slightly lower operation in the face of cyber-physical threats of individual agents.

In view of long-term utilization or environmentally affected components, MASs are vulnerable to physical anomaly problems, such as time-varying actuator faults (bias, partial loss of effectiveness, stuck or hard-over) [11], [12] and sensor faults (fixed deviation, drift deflection or accuracy degradation) [13], [14]. Compared to the handling of actuator or sensor faults individually [9], [15], the fault-tolerant consensus literature on the simultaneous dealing with actuator and sensor faults in the input and output channels of MASs is still relatively limited. Specifically, the enhanced resilient adaptive compensation protocol and H_∞ control strategies are proposed for MASs with local actuator and sensor faults [16]. The neuroadaptive inverse optimal consensus issue of uncertain high-order MASs [17] and distributed adaptive resilient consensus tracking issue of fuzzy-logic MASs [18] in the presence of actuator and sensor faults are investigated, respectively. On the one hand, the key feature is that the ever-developing consensus controller with compensa-

tion mechanisms is designed based on the full state of itself and neighboring state information [19], whereas the factors including output information or unavailable information estimated by observers [11], [12], [14] are rarely addressed in dealing with simultaneous actuator and sensor faults of nonlinear MASs. On the other hand, most research concentrate on constant or sudden faults of additive and multiplicative types [6], [11], while ignoring the hidden faults, namely, incipient faults in the early stage. It is worth noting that the widespread damage of the whole MASs may be due to the insignificant deviations or fluctuations of the individual agents spreading to its neighbors through fragile and unreliable network interaction, thus eventually destroying the order and coordination of MAS. In addition, owning to the coexistence of the abrupt/incipient-type actuator/sensor faults and additive communication noises [19], [20] or input channel noises [21], the exact fault-tolerant consensus cannot be reached effectively. Therefore, even under the influence of unified time-varying abrupt and incipient actuator/sensor failures and channel noises simultaneously, it is meaningful but challenging to devise the novel observer-based fault-tolerant consensus control concept from estimated dynamics to tolerant systems to construct unmeasurable fault information of nonlinear MASs.

The safe and reliable operation and evolution of MASs are affected not only by physical faults occurring on local components but also by information interruptions or topology disruptions induced by cyber-attacks in hostile environments [22]. The consensus implementation of MASs requires independent autonomous intelligences to preserve accurate and continuous uninterrupted information interaction, while cyber-attacks carried out by a hostile adversary poses a severe threat to MASs, eventually undermining the basic coordination. To combat various malicious cyber-attacks, such as actuator/sensor attacks [23], deception attacks [24], false data-injection and replay attacks [25], denial-of-service (DoS) attacks [26] and intermittent attacks [27], the secure fault-tolerant consensus of the cyber-physical MASs with an anti-attack mechanism urgently needs to be explored. The average dwelling time (ADT) technique-based distributed consensus protocol is developed for layered MASs under attacks on topological edges to achieve the node-to-node synchronization [28]. One of the key issues aforementioned is how to guarantee the desirable safe and resilient consensus performance of each individual as well as the entire MASs when confronted with simultaneous faults and attacks. Recent development analysis and trends of physical safety and cyber security of MASs are briefly reviewed in [29]. In contrast

to anomaly detection and identification subject to physical faults and cyber-attacks in some existing studies [30], the distributed impulsive mechanism-based cooperative fault-tolerant control [31] or the event-triggered adaptive fault-tolerant pinning control [32] are incorporated into the consensus field to compensate for actuator faults in the physical layer and to resist deception attacks and aperiodic DoS attacks, respectively. Another DoS attacks in nonlinear MASs and interval type 2 fuzzy networked MASs against simultaneous actuator faults are also investigated through the adaptive fault-tolerant consensus control scheme [33] and the fault-tolerant containment control strategy [34] with combination of both switching concept and ADT mechanism. In particular, by using the existing graph theory and switching technology [35], [36], it is extremely challenging to achieve cyber-physical tolerance and security of multi-agent consensus that suffers from unified actuator/sensor faults and maintained/paralyzed connectivities of topologies affected by variation in the nodes of action, degree of action and duration of failures and attacks. To eliminate the adverse effects of them, this study explicitly addresses the leader-following consensus issue, whereas providing stringent and co-designed framework of normalization and estimation-based observer and distributed anti-attack fault-tolerant consensus control strategies for nonlinear MASs, in the presence of unified abrupt and incipient actuator/sensor faults, channel noises and topology switching (connectivity-maintained and connectivity-paralyzed attacks).

The following contributions of this study are summarized. 1) Unlike consensus of MASs in compensating individual physical faults [12], [17] or resisting independent cyber-attacks [31], the distributed anti-attack fault-tolerant consensus control policy attempts to synchronously address the self-dynamic large deviations subject to unified abrupt and incipient actuator/sensor faults and input/output channel noises in the physical layer as well as the maintained/paralyzed connectivities caused by connectivity-mixed attacks in the cyber layer, which have unexpectedly high levels of confidence. 2) Normalization and estimation-based observer technique is invoked to decouple the structure of the augmented multi-agent dynamics and overcome the deleterious effects raised by unknown state and fault observations. Instead of devising separated units for fault detection, identification, isolation and control in consensus control communities [7], [30], the duality and compromise between observation and control layers (tolerance to faults, resilience to attacks, and robustness to noises) are generated in an integrated framework. 3) The computation of the ADT constraint [28], [33]-[35] is avoided by choos-

ing appropriate attack indicators (attack frequency and activation rates), and finally the online updating relationship between the exponential leader-following consensus performance and less conservative dual attack indicators is established intuitively.

The remainder of this study is structured as follows. Preliminaries and problem formulation of MASs with actuator/sensor fault and connectivity-mixed attack modeling are presented in Section 2. Main results including normalization/estimation-based observer design and distributed anti-attack fault-tolerant consensus control design are developed in Section 3. Simulation results in Section 4 are illustrated to exemplify the effectiveness and merits of the proposed fault-tolerant consensus control algorithm. Section 5 finally concludes conclusions with potential future investigations.

2. Preliminaries and Problem Formulation

2.1. Graph theory

A directed and switching topology $\mathcal{G}_{\gamma(t)}$ is a pair $(\nu, \varepsilon, \mathcal{A}_{\gamma(t)})$, where $\nu = \{\nu_1, \nu_2, \cdots, \nu_N\}$ is a nonempty finite set of nodes, $\varepsilon \subseteq \nu \times \nu$ is a set of edges, and (ν_i, ν_j) is an edge that denotes an ordered pair of nodes ν_i, ν_j. Adjacency matrix of the switching topology $\mathcal{G}_{\gamma(t)}$ is denoted by $\mathcal{A}_{\gamma(t)} = [a_{ij}^{\gamma(t)}] \in \mathbb{R}^{N\times N}$, where $a_{ij}^{\gamma(t)}$ is the weight coefficient of edge (ν_i, ν_j) and $a_{ii}^{\gamma(t)} = 0, a_{ij}^{\gamma(t)} > 0$ if $(\nu_i, \nu_j) \in \varepsilon$, otherwise, $a_{ij}^{\gamma(t)} = 0$. The laplacian matrix is $\mathcal{L}_{\gamma(t)} = \mathcal{D}_{\gamma(t)} - \mathcal{A}_{\gamma(t)} = [l_{ij}^{\gamma(t)}] \in \mathbb{R}^{N\times N}$, where $\mathcal{D}_{\gamma(t)} = [d_{ii}^{\gamma(t)}] \in \mathbb{R}^{N\times N}$ is a diagonal matrix with $d_{ii}^{\gamma(t)} = \sum_{j=1}^{N} a_{ij}^{\gamma(t)}$.

The leader-following interaction matrix is denoted by $\mathcal{H}_{\gamma(t)} = \mathcal{L}_{\gamma(t)} + \mathcal{B}_{\gamma(t)}$, where $\mathcal{B}_{\gamma(t)} = \text{diag}\{b_1^{\gamma(t)}, \cdots, b_N^{\gamma(t)}\}$ with $b_i^{\gamma(t)}$ denoted as the information interaction between node ν_i and the leader. If $b_i^{\gamma(t)} = 1$, the node ν_i can reach the leader via a directed path, otherwise, $b_i^{\gamma(t)} = 0$.

2.2. Actuator and sensor fault modeling in MASs

The general nonlinear MASs with a group of one leader and N followers are considered. The nonlinear dynamics of the ith follower in the presence of actuator/sensor faults and channel noises are established as

$$\begin{cases} \dot{x}_i(t) = Ax_i(t) + Bu_i(t) + F_a f_{ai}(t) + \xi(x_i(t), t) + E_1\omega_{i1}(t) \\ y_i(t) = Cx_i(t) + F_s f_{si}(t) + E_2\omega_{i2}(t), i = 1, \cdots, N \end{cases} \tag{1}$$

where $x_i(t) \in \mathbb{R}^n, u_i(t) \in \mathbb{R}^m, y_i(t) \in \mathbb{R}^p$ and $\xi(x_i(t), t) \in \mathbb{R}^n$ denote the state, input, output and nonlinearity vectors, respectively, $\omega_{i1}(t) \in \mathbb{R}^{s_1}$ and $\omega_{i2}(t) \in \mathbb{R}^{s_2}$ denote the input and output channel noises, respectively, $f_{ai}(t) \in \mathbb{R}^{q_1}$ and $f_{si}(t) \in \mathbb{R}^{q_2}$ denote the actuator and sensor fault, respectively. Matrices A, B, C denote the system-described gains, E_1, E_2 denote the noise-described gains, and F_a, F_s denote the physical fault-described gains with appropriate and known dimensions.

Actuator and sensor faults: $f_{ai}(t) = [f_{ai}^1(t), \cdots, f_{ai}^{q_1}(t)]^T$ and $f_{si}(t) = [f_{si}^1(t), \cdots, f_{si}^{q_2}(t)]^T$ in (1) are denoted as the unified abrupt-type and incipient-type time-varying actuator and sensor faults with each element $f_{ai}^{\varrho}(t)$ and $f_{si}^{\varrho}(t)$ modeled as

$$\begin{cases} f_{ai}^{\varrho}(t) = \left(1 - e^{-\epsilon_a^{\varrho}\left(t - T_a^{\varrho}\right)}\right) \bar{f}_{ai}^{\varrho}, t \geq T_a^{\varrho}, \varrho = 1, \cdots, q_1 \\ f_{si}^{\varrho}(t) = \left(1 - e^{-\epsilon_s^{\varrho}\left(t - T_s^{\varrho}\right)}\right) \bar{f}_{si}^{\varrho}, t \geq T_s^{\varrho}, \varrho = 1, \cdots, q_2 \end{cases} \tag{2}$$

where $\bar{f}_{ai}^{\varrho}, \bar{f}_{si}^{\varrho}$ are the ϱth row elements of unknown constant fault bounds, $T_a^{\varrho}, T_s^{\varrho}$ are the fault occurrence time instants, and $\epsilon_a^{\varrho}, \epsilon_s^{\varrho}$ are the unknown decay rates. The modeled actuator and sensor faults are defined as incipient-type faults (*slow-varying decay rate*) when $\underline{\epsilon}_{a(s)} \leq \epsilon_{a(s)}^{\varrho} < \bar{\epsilon}_{a(s)}$ and abrupt-type faults (*quick-varying decay rate*) when $\epsilon_{a(s)}^{\varrho} \geq \bar{\epsilon}_{a(s)}$, respectively.

The nonlinear system of the leader (labeled as 0) is modeled as

$$\begin{cases} \dot{x}_0(t) = Ax_0(t) + Bu_0(t) + \xi(x_0(t), t) \\ y_0(t) = Cx_0(t) \end{cases} \tag{3}$$

where $x_0(t) \in \mathbb{R}^n, y_0(t) \in \mathbb{R}^p$ and $\xi(x_0(t), t) \in \mathbb{R}^n$ represent the available state, output vectors and intrinsic system nonlinearity of the leader, respectively. The control input $u_0(t) \in \mathbb{R}^m$ is designed as $u_0(t) = -K_x x_0(t)$ with the derived state-estimation gain $K_x \in \mathbb{R}^{m \times n}$.

Assumption 1: The pairs (A, B) and (A, C) are controllable and observable, respectively.

Assumption 2: (i) The unified abrupt-type and incipient-type actuator and sensor faults are differentiable after each fault occurrence instants. The lower and upper bounds of decay rates ϵ_a^{ϱ} and ϵ_s^{ϱ} are determined manually with the known positive scalars $\underline{\epsilon}_{a(s)}$ and $\bar{\epsilon}_{a(s)}$. (ii) The input and output channel noises are constrained within the known and positive upper bounds, i.e., $\|\omega_{i1}(t)\| \leq \bar{\omega}_{i1}$ and $\|\dot{\omega}_{i2}(t)\| \leq \bar{\omega}_{i2}$, respectively.

Assumption 3: The state-dependent system nonlinearity is satisfied with the Lipschitz condition, i.e., $\|\xi(x_i(t),t)-\xi(x_j(t),t)\| \leq \beta\|x_i(t)-x_j(t)\|, i,j = 0,1,\cdots,N$ with the Lipschitz scalar $\beta > 0$.

2.3. Connectivity-mixed attack modeling

The time-varying signal $\gamma(t) : [0,\infty) \to \Gamma = \{1,\cdots,r\}$ is introduced to denote each topology switching caused by cyber attacks. The set $\{\mathcal{G}_1,\cdots,\mathcal{G}_r\}$ denotes the switching topologies $\mathcal{G}_{\gamma(t)}$, and $\{\mathcal{H}_1,\cdots,\mathcal{H}_r\}$ denotes the leader-following interaction matrices $\mathcal{H}_{\gamma(t)}$ for $\gamma(t) \in \Gamma$. The switching sequence is denoted as $k \in \mathbb{N}$ over $[t_0,t)$. Consider that there exists an infinite sequence of uniformly bounded and non-overlapping time intervals $[t_k,t_{k+1})$, in which the topology is time-invariant and non-switching.

Connectivity-mixed attacks: The topologies affected by connectivity-mixed attacks present two consequences: network connectivity is maintained and paralyzed, respectively. On the one hand, the connectivity-maintained topology (removing or relinking edges *slightly*) still remains connected and contains a directed spanning tree with the leader as the root. On the other hand, the connectivity-paralyzed topology (removing or relinking edges *dramatically*) falls disconnected without a directed spanning tree but can be recovered into connectivity through the attack defense or repair mechanism. The signal $\gamma(t) \in \Gamma = \Gamma_m \cup \Gamma_p = \{1,\cdots,q,q+1,\cdots,r\}, r \geq 2$ is introduced for the switching topologies $\{\mathcal{G}_1,\cdots,\mathcal{G}_q,\mathcal{G}_{q+1},\cdots,\mathcal{G}_r\}$, where Γ_m and Γ_p are the sets of q connectivity-maintained topologies and $(r-q)$ connectivity-paralyzed topologies, respectively.

Definition 1: Denote the number of connectivity-mixed attacks as $N_\Gamma(t_0,t) = N_{\Gamma_m}(t_0,t)+N_{\Gamma_p}(t_0,t), \forall t > t_0 \geq 0$ with the numbers of connectivity-maintained/-paralyzed topologies $N_{\Gamma_m}(t_0,t)$ and $N_{\Gamma_p}(t_0,t)$, respectively. Denote $\mathcal{F}_\Gamma(t_0,t) = \frac{N_\Gamma(t_0,t)}{t-t_0}$ as the connectivity-mixed attack frequency over $[t_0,t)$.

Definition 2: Denote $\mathcal{R}_{\Gamma_m}(t_0,t) = \frac{T_m(t_0,t)}{t-t_0}, \gamma(t) \in \Gamma_m$ and $\mathcal{R}_{\Gamma_p}(t_0,t) = \frac{T_p(t_0,t)}{t-t_0}, \gamma(t) \in \Gamma_p$ as the connectivity-maintained/-paralyzed attack activation rates over $[t_0,t)$, where the total activation durations of connectivity-maintained/-paralyzed topologies $T_m(t_0,t)$ and $T_p(t_0,t)$ are expressed as

$$\begin{cases} T_m(t_0,t) = \sum_{k\in\mathbb{N},\gamma(t_k)\in\Gamma_m}(t_{k+1}-t_k) \\ T_p(t_0,t) = \sum_{k\in\mathbb{N},\gamma(t_k)\in\Gamma_p}(t_{k+1}-t_k) \end{cases} \tag{4}$$

Definition 3: The control objective in this study aims at designing the novel fault-tolerant consensus control for the modelled nonlinear MASs (1)

to compensate the actuator/sensor faults and channel noises in the physical layer and resist the connectivity-mixed attacks in the networked layer through a distributed anti-attack strategy. Specifically, the leader-following consensus $\|x_i(t) - x_0(t)\|^2 \leq \mu e^{-\lambda(t-t_0)}\|x_i(t_0) - x_0(t_0)\|^2, \forall t \geq t_0$ is achieved with the positive amplitude μ and positive decay rate λ.

Lemma 1: $\Upsilon_{\gamma(t)} = \Phi_{\gamma(t)}\mathcal{H}_{\gamma(t)} + \mathcal{H}_{\gamma(t)}^T\Phi_{\gamma(t)}$ is a symmetric positive-definite matrix with $\Phi_{\gamma(t)} = \text{diag}\{\phi_{\gamma(t),1}^{-1}, \cdots, \phi_{\gamma(t),N}^{-1}\}$ denoted as the diagonal positive-definite matrix, where $\phi_{\gamma(t),i}, i = 1, \cdots, N$ corresponds with the row element of vector $\phi_{\gamma(t)} = (\mathcal{H}_{\gamma(t)}^{-1})^T\mathbf{1}_N$ for $\gamma(t) \in \Gamma$.

Remark 1: Compared with communication noises [19], [20] and individual noises appearing in the input channel [21], or uncertain coupling nonlinearities [7] and membership functions-based parameter uncertainty nonlinearities [34], simultaneous input and output channel noises ω_{i1} and ω_{i2} are considered, assuming that actuator/sensor faults are modeled in a general exponential form in Assumption 2, while the modeled system nonlinear perturbation $\xi(x_i(t), t)$ in Assumption 3 is constrained within the Lipschitz condition, which is more general than the norm-bounded canonical constraint.

Remark 2: For attacks that actively bypass and evade the monitoring of anomaly attack surveillance mechanisms, the attack sequence is hidden and inescapable from the defender, and the networked graphs may be affected by switched and updated connectivity-maintained/-paralyzed topologies, ultimately leading to a severe disruption of the node-to-node consensus. Compared with network disconnections described by switching mechanisms [33] or semi-Markov chains with random topology switching [36], a switching signal version-based connectivity-maintained topologies and connectivity-paralyzed topologies are incorporated to simulate the connectivity-mixed attack phenomenon, corresponding to different scenarios: 1) with a directed spanning tree and 2) without a spanning tree. Furthermore, despite the fact that a malicious adversary may launch attacks of different durations and the defender may not be able to determine the true situation at each moment, it is common sense to require that the switching topologies or sequences $\mathcal{G}_{\gamma(t)}$ be deterministic and switching known by some intelligent device. Modelled connectivity-mixed attacks can be characterized by setting attack frequency and activation rate constraints under which the problem of fault-tolerant consensus control can still be guaranteed, despite receiving the dynamic effects of actuator/sensor failures, channel noise, and cyber-attacks.

3. Main Results

The control framework contains the normalization/estimation-based observer design and distributed anti-attack fault-tolerant consensus control design to address the connectivity-mixed attacks in the cyber layer and unified abrupt-/incipient-type actuator/sensor faults and channel noises in the physical layer, as shown in Figure 1.

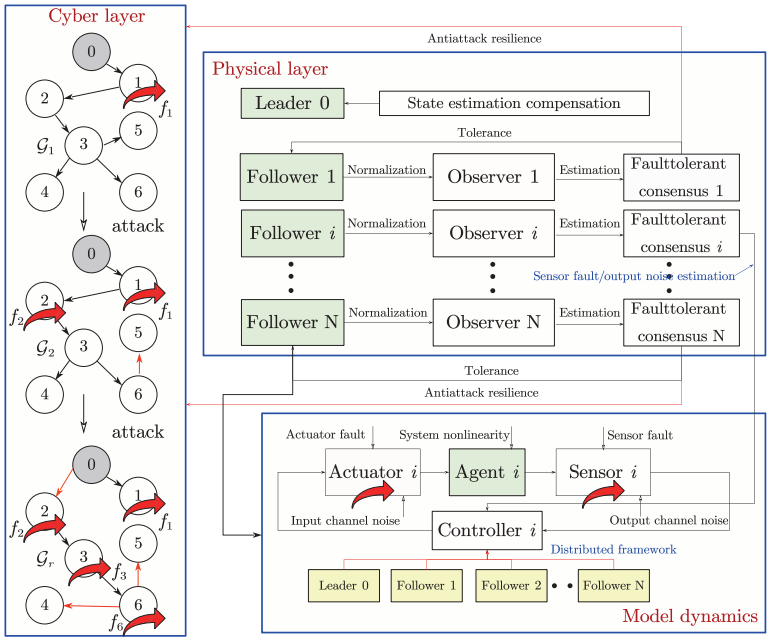

Figure 1: Control framework of cyber layer, physical layer and model dynamics.

3.1. Normalization and estimation-based observer design

For nonlinear MASs with mixed actuator/sensor faults and channel noises, the normalization of the derivable faults and noises into the same variable using augmented dimensionality techniques aims to hide the explicit system negative quantities of the input and output channels in the normalized state. This section exploits the intuitive estimation-based observer structure for the augmented system dynamics and supplements it with decoupled parameter designs so that only estimation error, augmented uncertainty and nonlinearity are decoupled from the estimation error dynamics. The innovative

observer framework thus enables efficient estimation of the original system state, actuator/sensor faults and output channel noises.

The normalization process of the original MASs (1) is formulated on the basis of the augmented state, uncertainty and nonlinearity items as follows

$$\begin{cases} \dot{\bar{x}}_i(t) = \bar{A}\bar{x}_i(t) + \bar{B}u_i(t) + \bar{D}\bar{d}_i(t) + \bar{\xi}(A_0\bar{x}_i(t), t) \\ y_i(t) = \bar{C}\bar{x}_i(t) \end{cases} \tag{5}$$

where $\bar{x}_i(t) = [x_i^T(t)\ \ f_{ai}^T(t)\ \ f_{si}^T(t)\ \ \omega_{i2}^T(t)]^T$ denotes the augmented state, $\bar{d}_i(t) = [\omega_{i1}^T(t)\ \ \dot{f}_{ai}^T(t)\ \ \dot{f}_{si}^T(t)\ \ \dot{\omega}_{i2}^T(t)]^T$ denotes the augmented uncertainty, $\bar{\xi}(A_0\bar{x}_i(t), t) = [\xi^T(x_i(t), t)\ \mathbf{0}_{1\times q_1}\ \mathbf{0}_{1\times q_2}\ \mathbf{0}_{1\times s_2}]^T$ denotes the augmented nonlinearity with $A_0 = [I_n\ \mathbf{0}_{n\times q_1}\ \mathbf{0}_{n\times q_2}\ \mathbf{0}_{n\times s_2}]$, and the system matrices $\bar{A}, \bar{B}, \bar{D}$ and $\bar{C}$ are expressed as

$$\begin{aligned} \bar{A} &= \begin{bmatrix} A & F_a & \mathbf{0}_{n\times q_2} & \mathbf{0}_{n\times s_2} \\ \mathbf{0}_{q_1\times n} & \mathbf{0}_{q_1\times q_1} & \mathbf{0}_{q_1\times q_2} & \mathbf{0}_{q_1\times s_2} \\ \mathbf{0}_{q_2\times n} & \mathbf{0}_{q_2\times q_1} & \mathbf{0}_{q_2\times q_2} & \mathbf{0}_{q_2\times s_2} \\ \mathbf{0}_{s_2\times n} & \mathbf{0}_{s_2\times q_1} & \mathbf{0}_{s_2\times q_2} & \mathbf{0}_{s_2\times s_2} \end{bmatrix}, \bar{B} = \begin{bmatrix} B \\ \mathbf{0}_{q_1\times m} \\ \mathbf{0}_{q_2\times m} \\ \mathbf{0}_{s_2\times m} \end{bmatrix} \\ \bar{D} &= \begin{bmatrix} E_1 & \mathbf{0}_{n\times q_1} & \mathbf{0}_{n\times q_2} & \mathbf{0}_{n\times s_2} \\ \mathbf{0}_{q_1\times s_1} & I_{q_1} & \mathbf{0}_{q_1\times q_2} & \mathbf{0}_{q_1\times s_2} \\ \mathbf{0}_{q_2\times s_1} & \mathbf{0}_{q_2\times q_1} & I_{q_2} & \mathbf{0}_{q_2\times s_2} \\ \mathbf{0}_{s_2\times s_1} & \mathbf{0}_{s_2\times q_1} & \mathbf{0}_{s_2\times q_2} & I_{s_2} \end{bmatrix}, \bar{C} = \begin{bmatrix} C^T \\ \mathbf{0}_{q_1\times p} \\ F_s^T \\ E_2^T \end{bmatrix}^T \end{aligned} \tag{6}$$

Define the augmented state estimation as $\hat{\bar{x}}_i(t) = z_i(t) + Hy_i(t)$ with $\hat{\bar{x}}_i(t) = [\hat{x}_i^T(t)\ \hat{f}_{ai}^T(t)\ \hat{f}_{si}^T(t)\ \hat{\omega}_{i2}^T(t)]^T$ denoted as the estimation of $\bar{x}_i(t)$, where $\hat{x}_i(t) \in \mathbb{R}^n$, $\hat{f}_{ai}(t) \in \mathbb{R}^{q_1}$, $\hat{f}_{si}(t) \in \mathbb{R}^{q_2}$ and $\hat{\omega}_{i2}(t) \in \mathbb{R}^{s_2}$ denote the respective estimated state, actuator fault, sensor fault and output channel noise vectors. Then, the augmented estimation-based observer is devised for the normalized structure (5) as follows

$$\dot{z}_i(t) = (\Theta\bar{A} - J_1\bar{C})z_i(t) + \Theta\bar{B}u_i(t) + (J_1 + J_2)y_i(t) + \Theta\bar{\xi}(A_0\hat{\bar{x}}_i(t), t) \tag{7}$$

where $z_i(t) \in \mathbb{R}^{n+q_1+q_2+s_2}$ is the designed observer's state, $\bar{\xi}(A_0\hat{\bar{x}}_i(t), t) = [\xi^T(\hat{x}_i(t), t)\ \mathbf{0}_{1\times q_1}\ \mathbf{0}_{1\times q_2}\ \mathbf{0}_{1\times s_2}]^T$, and Θ, J_1, J_2 are later devised matrices of proper dimensions.

Subsequently, define the augmented estimation error as $e_{i1}(t) = \bar{x}_i(t) - \hat{\bar{x}}_i(t) = [e_{xi}^T(t)\ e_{ai}^T(t)\ e_{si}^T(t)\ e_{\omega i}^T(t)]^T$ with the state estimation error $e_{xi}(t) = x_i(t) - \hat{x}_i(t)$, the actuator fault estimation error $e_{ai}(t) = f_{ai}(t) - \hat{f}_{ai}(t)$, the sensor fault estimation error $e_{si}(t) = f_{si}(t) - \hat{f}_{si}(t)$ and the output channel

noise estimation error $e_{\omega i}(t) = \omega_{i2}(t) - \hat{\omega}_{i2}(t)$. Then, the augmented estimation error dynamics are obtained as

$$\begin{aligned}\dot{e}_{i1}(t) = &\left(\Theta\bar{A} - J_1\bar{C}\right)e_{i1}(t) + \left(\left(\Theta\bar{A} - J_1\bar{C}\right)H - J_2\right)y_i(t) \\ &+\Theta\left(\bar{\xi}(A_0\bar{x}_i(t),t) - \bar{\xi}(A_0\hat{\bar{x}}_i(t),t)\right) + \Theta\bar{D}\bar{d}_i(t)\end{aligned} \tag{8}$$

In order to decouple the additional output item in the augmented estimation error dynamics (8), matrices $\Theta = \mathcal{I} - H\bar{C}$ and $J_2 = \bar{A}H - H\bar{C}\bar{A}H - J_1\bar{C}H$ are defined with $\mathcal{I} = I_{n+q_1+q_2+s_2}$. Then, it follows that

$$\begin{aligned}\dot{e}_{i1}(t) = &\left(\bar{A} - H\bar{C}\bar{A} - J_1\bar{C}\right)e_{i1}(t) + \left(\bar{D} - H\bar{C}\bar{D}\right)\bar{d}_i(t) \\ &+\left(\mathcal{I} - H\bar{C}\right)\Delta\bar{\xi}_i(t)\end{aligned} \tag{9}$$

where the nonlinear estimation error is $\Delta\bar{\xi}_i(t) = \bar{\xi}(A_0\bar{x}_i(t),t) - \bar{\xi}(A_0\hat{\bar{x}}_i(t),t)$.

The augmented estimation error dynamics with the global formulation $e_1(t) = [e_{11}^T(t), \cdots, e_{N1}^T(t)]^T$ are derived as follows

$$\begin{aligned}\dot{e}_1(t) = &\left(I_N \otimes \left(\bar{A} - H\bar{C}\bar{A} - J_1\bar{C}\right)\right)e_1(t) + \left(I_N \otimes \left(\bar{D} - H\bar{C}\bar{D}\right)\right)\bar{d}(t) \\ &+\left(I_N \otimes \left(\mathcal{I} - H\bar{C}\right)\right)\Delta\bar{\xi}(t)\end{aligned} \tag{10}$$

where $\bar{d}(t) = [\bar{d}_1^T(t), \cdots, \bar{d}_N^T(t)]^T$ and $\Delta\bar{\xi}(t) = [\Delta\bar{\xi}_1^T(t), \cdots, \Delta\bar{\xi}_N^T(t)]^T$.

Thus, the observer design based on normalization and estimation decomposes essentially into solving the matrices H and J_1 such that the augmented estimation error dynamics (9) and (10) are robustly asymptotically stable, i.e., the state estimation $\hat{x}_i(t) \to x_i(t)$, the actuator/sensor fault estimations $\hat{f}_{ai}(t) \to f_{ai}(t)$, $\hat{f}_{si}(t) \to f_{si}(t)$ and the derivative output channel noise estimation $\hat{\omega}_{i2}(t) \to \omega_{i2}(t)$ when $t \to +\infty$.

3.2. Distributed anti-attack fault-tolerant consensus control design

The motivation of the distributed anti-attack fault-tolerant consensus control design of MASs in this section is achieved in three main ways. First, the fault-tolerant controller contains robust compensation for the unified actuator/sensor faults in the physical layer. Second, the anti-attack controller with strong resistance contains topological information based on switching signals against connectivity-mixed attacks in the cyber layer. Third, the distributed structure in the consensus controller on the basis of leader-following interaction-based output information, estimated sensor fault and derivative output channel noise collections is proposed for efficient and timely convergence of the leader-following tracking performance.

The anti-attack fault-tolerant consensus controller of the ith follower in MASs under actuator/sensor faults, channel noises and connectivity-mixed attacks with a distributed structure is designed as

$$\begin{aligned} u_i(t) = &-K\hat{\bar{x}}_i(t) + \delta R(\textstyle\sum_{j=1}^{N} a_{ij}^{\gamma(t)}(y_j(t) - y_i(t)) + b_i^{\gamma(t)}(y_0(t) - y_i(t))) \\ &+\delta RF_s\left(\textstyle\sum_{j=1}^{N} a_{ij}^{\gamma(t)}(\hat{f}_{sj}(t) - \hat{f}_{si}(t)) - b_i^{\gamma(t)}\hat{f}_{si}(t)\right) \\ &+\delta RE_2\left(\textstyle\sum_{j=1}^{N} a_{ij}^{\gamma(t)}(\hat{\omega}_{j2}(t) - \hat{\omega}_{i2}(t)) - b_i^{\gamma(t)}\hat{\omega}_{i2}(t)\right) \end{aligned} \tag{11}$$

where $K = [K_x \ K_a \ \mathbf{0}_{m\times q_2} \ \mathbf{0}_{m\times s_2}]$ denotes the compensation gain with the state-estimation gain $K_x \in \mathbb{R}^{m\times n}$ and actuator fault-estimation gain $K_a = B^{\dagger}F_a \in \mathbb{R}^{m\times q_1}$, R is the coupling matrix, $\delta > 0$ is the coupling coefficient, $a_{ij}^{\gamma(t)}$ is the (i,j)th coefficient between the ith and jth followers corresponding with the switching topology $\mathcal{G}_{\gamma(t)}$, and $b_i^{\gamma(t)} = 1$ when the ith follower can access the leader and $b_i^{\gamma(t)} = 0$, otherwise.

Define the leader-following consensus error as $e_{i2}(t) = x_i(t) - x_0(t)$. The corresponding leader-following consensus error dynamics are derived as

$$\begin{aligned} \dot{e}_{i2}(t) = &(A - BK_x)e_{i2}(t) + BKe_{i1}(t) + E_1\omega_{i1}(t) + \xi(x_i(t),t) \\ &-\xi(x_0(t),t) + \delta BR\left(\textstyle\sum_{j=1}^{N} a_{ij}^{\gamma(t)}\left(y_j(t) - y_i(t)\right) + b_i^{\gamma(t)}\left(y_0(t) - y_i(t)\right)\right) \\ &+\delta BRF_s\left(\textstyle\sum_{j=1}^{N} a_{ij}^{\gamma(t)}\left(\hat{f}_{sj}(t) - \hat{f}_{si}(t)\right) - b_i^{\gamma(t)}\hat{f}_{si}(t)\right) \\ &+\delta BRE_2\left(\textstyle\sum_{j=1}^{N} a_{ij}^{\gamma(t)}(\hat{\omega}_{j2}(t) - \hat{\omega}_{i2}(t)) - b_i^{\gamma(t)}\hat{\omega}_{i2}(t)\right) \\ = &(A - BK_x)e_{i2}(t) + BKe_{i1}(t) + E_1\omega_{i1}(t) + e_{\xi i}(t) \\ &+\delta BRC\left(\textstyle\sum_{j=1}^{N} a_{ij}^{\gamma(t)}\left(e_{j2}(t) - e_{i2}(t)\right) - b_i^{\gamma(t)}e_{i2}(t)\right) \\ &+\delta BRF_s\left(\textstyle\sum_{j=1}^{N} a_{ij}^{\gamma(t)}\left(e_{sj}(t) - e_{si}(t)\right) - b_i^{\gamma(t)}e_{si}(t)\right) \\ &+\delta BRE_2\left(\textstyle\sum_{j=1}^{N} a_{ij}^{\gamma(t)}\left(e_{\omega j}(t) - e_{\omega i}(t)\right) - b_i^{\gamma(t)}e_{\omega i}(t)\right) \end{aligned} \tag{12}$$

where the leader-following nonlinear tracking error is denoted as $e_{\xi i}(t) = \xi(x_i(t),t) - \xi(x_0(t),t)$.

Then, the global consensus error dynamics are given as

$$\begin{aligned} \dot{e}_2(t) = &\left(I_N \otimes (A - BK_x) - \delta\left(\mathcal{H}_{\gamma(t)} \otimes BRC\right)\right)e_2(t) \\ &+ \left(I_N \otimes BK\right)e_1(t) + e_{\xi}(t) + \left(I_N \otimes E_1\right)\omega_1(t) \\ &-\delta\left(\mathcal{H}_{\gamma(t)} \otimes BRF_s\right)e_s(t) - \delta\left(\mathcal{H}_{\gamma(t)} \otimes BRE_2\right)e_{\omega}(t) \\ = &\left(I_N \otimes (A - BK_x) - \delta\left(\mathcal{H}_{\gamma(t)} \otimes BRC\right)\right)e_2(t) \\ &+ \left(I_N \otimes BK - \delta\left(\mathcal{H}_{\gamma(t)} \otimes BRF_sE_s\right) - \delta\left(\mathcal{H}_{\gamma(t)} \otimes BRE_2E_{\omega}\right)\right)e_1(t) \\ &+e_{\xi}(t) + \left(I_N \otimes E_1\right)\omega_1(t) \end{aligned} \tag{13}$$

where $\mathcal{H}_{\gamma(t)}$ denotes the nonsingular leader-following interaction matrix, $e_2(t) = [e_{12}^T(t), \cdots, e_{N2}^T(t)]^T, e_\xi(t) = [e_{\xi 1}^T(t), \cdots, e_{\xi N}^T(t)]^T, \omega_1(t) = [\omega_{11}^T(t), \cdots, \omega_{N1}^T(t)]^T$, $e_s(t) = [e_{s1}^T(t), \cdots, e_{sN}^T(t)]^T$ and $e_\omega(t) = [e_{\omega 1}^T(t), \cdots, e_{\omega N}^T(t)]^T$. The transformed matrices are $E_s = [\mathbf{0}_{q_2\times n}\ \mathbf{0}_{q_2\times q_1}\ I_{q_2}\ \mathbf{0}_{q_2\times s_2}], E_\omega = [\mathbf{0}_{s_2\times n}\ \mathbf{0}_{s_2\times q_1}\ \mathbf{0}_{s_2\times q_2}\ I_{s_2}]$.

The following sufficient condition is developed for the modeled nonlinear MASs (1) and (3) in the presence of the unified abrupt-/incipient-type actuator/sensor faults and channel noises in the physical layer as well as hostile connectivity-mixed attacks in the cyber layer through an integration of the normalization and estimation-based observer and distributed anti-attack fault-tolerant consensus control strategies.

Theorem 1: Given positive scalars $\chi_1, \chi_2, \chi_3, \chi_4, \sigma_\Gamma$ and δ_0, the leader-following MASs (1) and (3) with the framework of the normalization and estimation-based observer design (7) and the distributed anti-attack fault-tolerant consensus control protocol (11) can achieve the exponential consensus tracking performance in Definition 3, if there exists a symmetric positive-definite matrix $P \in \mathbb{R}^{n\times n}$, matrices $K_x \in \mathbb{R}^{m\times n}, H \in \mathbb{R}^{(n+q_1+q_2+s_2)\times p}, J_1 \in \mathbb{R}^{(n+q_1+q_2+s_2)\times p}$ and positive scalars τ_1, τ_2, τ_3 such that

$$\begin{aligned}&\chi_1\left(\mathrm{He}[(A-BK_x)^TP] + E_1E_1^T + I_n + \beta^2P^2\right)\\ &< \chi_1\chi_3 P < \chi_3\left(\mathrm{He}[(BK_x - A)^TP] - \varphi_{\max}(\lambda_2 E_1E_1^T + \lambda_2 I_n + P^2)\right)\end{aligned} \tag{14}$$

$$\begin{aligned}&\tfrac{1}{\tau_1}(\mathrm{He}[\bar{A} - H\bar{C}\bar{A} - J_1\bar{C}] + (\bar{D} - H\bar{C}\bar{D})(\bar{D} - H\bar{C}\bar{D})^T + (\mathcal{I} - H\bar{C})(\mathcal{I} - H\bar{C})^T\\ &+\beta^2 A_0^TA_0) + K^TK - \delta(E_s^TF_s^TR^TRF_sE_s + E_\omega^TE_2^TR^TRE_2E_\omega) + \chi_2\mathcal{I} < 0\end{aligned} \tag{15}$$

$$\begin{aligned}&\max\left(\tfrac{\epsilon_a}{\chi_2} - \sqrt{\tfrac{\epsilon_a^2}{\chi_2^2} - \tfrac{\tau_2}{\chi_2}}, \tfrac{\epsilon_s}{\chi_2} - \sqrt{\tfrac{\epsilon_s^2}{\chi_2^2} - \tfrac{\tau_3}{\chi_2}}\right) < \tau_1\\ &\le \min\left(\tfrac{\epsilon_a}{\chi_2} + \sqrt{\tfrac{\epsilon_a^2}{\chi_2^2} - \tfrac{\tau_2}{\chi_2}}, \tfrac{\epsilon_s}{\chi_2} + \sqrt{\tfrac{\epsilon_s^2}{\chi_2^2} - \tfrac{\tau_3}{\chi_2}}\right)\end{aligned} \tag{16}$$

$$0 < \tau_2 \le \tfrac{\epsilon_a^2}{\chi_2}, 0 < \tau_3 \le \tfrac{\epsilon_s^2}{\chi_2} \tag{17}$$

$$\max(\chi_3, \chi_4\tau_1) \ge \min(\chi_1, \chi_2\tau_1) \tag{18}$$

where the lower bounds $\underline{\epsilon}_a = \min_{\varrho=v,r,p} \epsilon_a^\varrho, \underline{\epsilon}_s = \min_{\varrho=1,2} \epsilon_s^\varrho, \lambda_2 = \lambda_{\max}(\Upsilon_{\gamma(t)}^2)$, and $\varphi_{\max} = \max_{i=1,\cdots,N} \varphi_{\gamma(t),i}, \gamma(t) \in \Gamma_m$.

The coupling matrix and coupling coefficient in the distributed anti-attack fault-tolerant consensus controller (11) are devised as $R = B^TP^{-1}C^\dagger$ and $\delta = \max\{\frac{\lambda_2}{\lambda_1+2\lambda_3}, \frac{1}{2\lambda_4(1+\lambda_4)}\} + \delta_0$ with a preset positive scalar δ_0 and another scalars denoted as $\lambda_1 = \lambda_{\min}(\mathrm{He}[\Upsilon_{\gamma(t)}\mathcal{H}_{\gamma(t)}]), \lambda_3 = \lambda_{\min}(\Upsilon_{\gamma(t)}\mathcal{H}_{\gamma(t)}\mathcal{H}_{\gamma(t)}^T\Upsilon_{\gamma(t)})$ for $\gamma(t) \in \Gamma_m$, and $\lambda_4 = \lambda_{\min}(\mathcal{H}_{\gamma(t)})$ for $\gamma(t) \in \Gamma_p$.

For a positive decay rate $\rho_\Gamma \in (0, \rho^\star)$ with the selected positive scalar $\rho^\star \in (0, \eta_m), \eta_m = \min(\chi_1, \chi_2\tau_1)$, the connectivity-mixed attack frequency $\mathcal{F}_\Gamma(t_0, t)$ satisfies with

$$\mathcal{F}_\Gamma(t_0, t) \leq \ln^{-1}\left(\frac{N\overline{\varphi}}{\tau_1\underline{\varphi}}\left((1+\tau_1)\bar{\omega}_1^2 + \bar{\omega}_2^2\right)\right)(\rho^\star - \rho_\Gamma) \tag{19}$$

and each connectivity-maintained/-paralyzed attack activation rates $\mathcal{R}_{\Gamma_m}(t_0, t)$ and $\mathcal{R}_{\Gamma_p}(t_0, t)$ over $[t_0, t)$ constrain within

$$\mathcal{R}_{\Gamma_m}(t_0, t) \geq \frac{\eta_p + \rho^\star}{\eta_m + \eta_p}, \mathcal{R}_{\Gamma_p}(t_0, t) \leq \frac{\eta_m - \rho^\star}{\eta_m + \eta_p} \tag{20}$$

where $\eta_p = \max(\chi_3, \chi_4\tau_1), \bar{\omega}_1 = \max\limits_{i=1,\cdots,N} \bar{\omega}_{i1}, \bar{\omega}_2 = \max\limits_{i=1,\cdots,N} \bar{\omega}_{i2}, \underline{\varphi} = \min\limits_{i=1,\cdots,N} \varphi_{\gamma(t),i}$, and $\overline{\varphi} = \max\limits_{i=1,\cdots,N} \varphi_{\gamma(t),i}$ for $\gamma(t) \in \Gamma_m$.

Hence, the leader-following consensus control issue of the considered nonlinear MASs in the presence of actuator/sensor faults and channel noises in the physical layer as well as connectivity-mixed attacks in the cyber layer is addressed with the following exponential consensus error expression

$$\|x_i(t) - x_0(t)\|^2 \leq \mu_\Gamma e^{-\rho_\Gamma(t-t_0)}\|x_i(t_0) - x_0(t_0)\|^2 \tag{21}$$

with the decay rate ρ_Γ and the amplitude scalar μ_Γ expressed as

$$\mu_\Gamma = \frac{N((1+\tau_1)\bar{\omega}_1^2 + \bar{\omega}_2^2)\left(\max\left(\lambda_{\max}(\varphi_{\gamma(t),i}^{-1}P^{-1}), \lambda_{\max}(P^{-1})\right) + \sigma_\Gamma\right)}{\tau_1 \min\left(\lambda_{\min}(\varphi_{\gamma(t),i}^{-1}P^{-1}), \lambda_{\min}(P^{-1})\right)} \tag{22}$$

Proof. Consider the following piece-wise Lyapunov function $V_1(t) = V_1^m(t)$ for $\gamma(t) \in \Gamma_m$ and $V_1(t) = V_1^p(t)$ for $\gamma(t) \in \Gamma_p$,

$$\begin{cases} V_1^m(t) = \sum_{i=1}^N e_{i2}^T(t)\varphi_{\gamma(t),i}^{-1}P^{-1}e_{i2}(t), \gamma(t) \in \Gamma_m \\ V_1^p(t) = \sum_{i=1}^N e_{i2}^T(t)P^{-1}e_{i2}(t), \gamma(t) \in \Gamma_p \end{cases} \tag{23}$$

where P denotes the symmetric positive-definite matrix and $\varphi_{\gamma(t),i}^{-1}, \gamma(t) \in \Gamma_m, i = 1, \cdots, N$ is the element scalar of the diagonal positive-definite matrix $\Upsilon_{\gamma(t)}$ in Lemma 1.

Introduce the new vector $\vartheta(t) = [\vartheta_1^T(t), \cdots, \vartheta_N^T(t)]^T$ with each element $\vartheta_i(t) = P^{-1}e_{i2}(t)$. According to the coupling matrix $R = B^TP^{-1}C^\dagger$, the

derivative of the Lyapunov function $V_1^m(t)$ when $\gamma(t) \in \Gamma_m$ is obtained as

$$\begin{aligned}
\dot{V}_1^m &= 2\sum_{i=1}^N \vartheta_i^T \varphi_{\gamma(t),i}^{-1}(A-BK_x)P\vartheta_i + 2\sum_{i=1}^N \vartheta_i^T \varphi_{\gamma(t),i}^{-1} BKe_{i1} \\
&\quad +2\sum_{i=1}^N \vartheta_i^T \varphi_{\gamma(t),i}^{-1} E_1\omega_{i1} + 2\sum_{i=1}^N \vartheta_i^T \varphi_{\gamma(t),i}^{-1} e_{\xi i} \\
&\quad +2\delta\sum_{i=1}^N \vartheta_i^T \varphi_{\gamma(t),i}^{-1} BB^T\left(\sum_{j=1}^N a_{ij}^{\gamma(t)}(\vartheta_j-\vartheta_i) - b_i^{\gamma(t)}\vartheta_i\right) \\
&\quad +2\delta\sum_{i=1}^N \vartheta_i^T \varphi_{\gamma(t),i}^{-1} BR(F_sE_s+E_2E_\omega)\left(\sum_{j=1}^N a_{ij}^{\gamma(t)}(e_{j1}-e_{i1}) - b_i^{\gamma(t)}e_{i1}\right) \\
&= \vartheta^T(\Upsilon_{\gamma(t)} \otimes \mathrm{He}[(A-BK_x)P])\vartheta - \delta\vartheta^T(\mathrm{He}[\Upsilon_{\gamma(t)}\mathcal{H}_{\gamma(t)}] \otimes BB^T)\vartheta \\
&\quad +2\sum_{i=1}^N \vartheta_i^T \varphi_{\gamma(t),i}^{-1} E_1\omega_{i1} + 2\sum_{i=1}^N \vartheta_i^T \varphi_{\gamma(t),i}^{-1} e_{\xi i} \\
&\quad +2\vartheta^T(\Upsilon_{\gamma(t)} \otimes BK - \delta\Upsilon_{\gamma(t)}\mathcal{H}_{\gamma(t)} \otimes BR(F_sE_s+E_2E_\omega))e_1 \\
&\le \vartheta^T\left(\Upsilon_{\gamma(t)} \otimes \mathrm{He}\left[(A-BK_x)P\right]\right)\vartheta - \delta\lambda_1\vartheta^T\left(I_N\otimes BB^T\right)\vartheta + \omega_1^T\omega_1 \\
&\quad +\lambda_2\vartheta^T\left(I_N\otimes E_1E_1^T\right)\vartheta + \lambda_2\vartheta^T\left(I_N\otimes BB^T\right)\vartheta - 2\delta\lambda_3\vartheta^T(I_N\otimes BB^T)\vartheta \\
&\quad +e_1^T(I_N\otimes(K^TK - \delta E_s^TF_s^TR^TRF_sE_s - \delta E_\omega^TE_2^TR^TRE_2E_\omega))e_1 \\
&\quad +\lambda_2\vartheta^T\vartheta + \beta^2\vartheta^T(I_N\otimes P^2)\vartheta \\
&\le \vartheta^T\left(\Upsilon_{\gamma(t)} \otimes \left(\mathrm{He}\left[(A-BK_x)P\right] + \varphi_{\max}(\lambda_2E_1E_1^T + \lambda_2I_n + P^2)\right)\right)\vartheta \\
&\quad +\omega_1^T\omega_1 + e_1^T\left(I_N\otimes\left(K^TK - \delta E_s^TF_s^TR^TRF_sE_s - \delta E_\omega^TE_2^TR^TRE_2E_\omega\right)\right)e_1
\end{aligned} \tag{24}$$

where the nonlinear tracking error is satisfied with $\|e_{\xi i}(t)\| \le \beta\|e_{i2}(t)\|$ and $e_\xi^T(t)e_\xi(t) \le \sum_{i=1}^N \beta^2 e_{i2}^T(t)e_{i2}(t)$, and the coupling coefficient is constrained within $\delta \ge \frac{\lambda_2}{\lambda_1+2\lambda_3}$ with $\lambda_1 = \lambda_{\min}(\mathrm{He}[\Upsilon_{\gamma(t)}\mathcal{H}_{\gamma(t)}]), \lambda_2 = \lambda_{\max}(\Upsilon_{\gamma(t)}^2), \lambda_3 = \lambda_{\min}(\Upsilon_{\gamma(t)}\mathcal{H}_{\gamma(t)}\mathcal{H}_{\gamma(t)}^T\Upsilon_{\gamma(t)})$, and $\varphi_{\max} = \max\limits_{i=1,\cdots,N}\varphi_{\gamma(t),i}, \gamma(t) \in \Gamma_m$.

Meanwhile, the derivative of the Lyapunov function $V_1^p(t)$ (23) when $\gamma(t) \in \Gamma_p$ is obtained as

$$\begin{aligned}
\dot{V}_1^p &\le \vartheta^T\left(I_N\otimes \mathrm{He}\left[(A-BK_x)P\right]\right)\vartheta + \vartheta^T\left(I_N\otimes E_1E_1^T\right)\vartheta + \omega_1^T\omega_1 \\
&\quad -2\delta\vartheta^T(\mathcal{H}_{\gamma(t)}\otimes BB^T)\vartheta + \vartheta^T\left(I_N\otimes BB^T\right)\vartheta + e_1^T\left(I_N\otimes K^TK\right)e_1 \\
&\quad -2\delta\vartheta^T(\mathcal{H}_{\gamma(t)}\mathcal{H}_{\gamma(t)}^T\otimes BB^T)\vartheta - \delta e_1^T\left(I_N\otimes E_s^TF_s^TR^TRF_sE_s\right)e_1 \\
&\quad -\delta e_1^T\left(I_N\otimes E_\omega^TE_2^TR^TRE_2E_\omega\right)e_1 + 2\sum_{i=1}^N \vartheta_i^Te_{\xi i} \\
&\le \vartheta^T\left(I_N\otimes \mathrm{He}\left[(A-BK_x)P\right]\right)\vartheta + \vartheta^T\left(I_N\otimes E_1E_1^T\right)\vartheta + \omega_1^T\omega_1 \\
&\quad +\vartheta^T\vartheta + e_2^T(I_N\otimes\beta^2I_n)e_2 + (-2\sigma\lambda_4 - 2\sigma\lambda_4^2 + 1)\vartheta^T(I_N\otimes BB^T)\vartheta \\
&\quad +e_1^T\left(I_N\otimes(K^TK - \delta E_s^TF_s^TR^TRF_sE_s - \delta E_\omega^TE_2^TR^TRE_2E_\omega)\right)e_1 \\
&\le \vartheta^T\left(I_N\otimes\left(\mathrm{He}\left[(A-BK_x)P\right] + E_1E_1^T + I_n + \beta^2P^2\right)\right)\vartheta + \omega_1^T\omega_1 \\
&\quad +e_1^T\left(I_N\otimes(K^TK - \delta E_s^TF_s^TR^TRF_sE_s - \delta E_\omega^TE_2^TR^TRE_2E_\omega)\right)e_1
\end{aligned} \tag{25}$$

where the coupling coefficient is also constrained within $\delta \ge \frac{1}{2\lambda_4(1+\lambda_4)}$ with $\lambda_4 = \lambda_{\min}(\mathcal{H}_{\gamma(t)}), \gamma(t) \in \Gamma_p$.

Subsequently, consider another Lyapunov function $V_2(t)$ that combines the augmented estimation error $e_{i1}(t)$ with the uniform derivative type for

abrupt and incipient actuator/sensor faults $\dot{f}_{ai}(t), \dot{f}_{si}(t)$ as follows

$$V_2(t) = \sum_{i=1}^{N} \left(\frac{1}{\tau_1} e_{i1}^T(t) e_{i1}(t) + \frac{1}{\tau_2} \dot{f}_{ai}^T(t) \dot{f}_{ai}(t) + \frac{1}{\tau_3} \dot{f}_{si}^T(t) \dot{f}_{si}(t) \right) \tag{26}$$

with scalars $\tau_1 > 0, \tau_2 > 0$ and $\tau_3 > 0$.

Before deriving the derivative of $V_2(t)$ in (26), the relationship of the first-order and second-order derivatives of unified abrupt-type and incipient-type actuator and sensor faults $f_{\delta i}^{\varrho}(t)$ and $f_{si}^{\varrho}(t)$ is modeled as an exponentially varying characteristic,

$$\begin{cases} \ddot{f}_{ai}^{\varrho}(t) = -(\epsilon_a^{\varrho})^2 e^{-\epsilon_a^{\varrho}(t-T_a^{\varrho})} \bar{f}_{ai}^{\varrho} = -\epsilon_a^{\varrho} \dot{f}_{ai}^{\varrho}(t), \varrho = 1, \cdots, q_1 \\ \ddot{f}_{si}^{\varrho}(t) = -(\epsilon_s^{\varrho})^2 e^{-\epsilon_s^{\varrho}(t-T_s^{\varrho})} \bar{f}_{si}^{\varrho} = -\epsilon_s^{\varrho} \dot{f}_{si}^{\varrho}(t), \varrho = 1, \cdots, q_2 \end{cases} \tag{27}$$

Then, the derivative of the Lyapunov function $V_2(t)$ (26) is derived as

$$\begin{aligned} \dot{V}_2 &= \tfrac{1}{\tau_1} \textstyle\sum_{i=1}^{N} e_{i1}^T (\mathrm{He}[\bar{A} - H\bar{C}\bar{A} - J_1\bar{C}] + (\bar{D} - H\bar{C}\bar{D})(\bar{D} - H\bar{C}\bar{D})^T \\ &\quad + (\mathcal{I} - H\bar{C})(\mathcal{I} - H\bar{C})^T) e_{i1} + \tfrac{1}{\tau_1} \textstyle\sum_{i=1}^{N} \Delta\bar{\xi}_i^T \Delta\bar{\xi}_i + \tfrac{2}{\tau_2} \textstyle\sum_{i=1}^{N} \dot{f}_{ai}^T \ddot{f}_{ai} \\ &\quad + \tfrac{1}{\tau_1} \textstyle\sum_{i=1}^{N} \left(\omega_{i1}^T \omega_{i1} + \dot{f}_{ai}^T \dot{f}_{ai} + \dot{f}_{si}^T \dot{f}_{si} + \dot{\omega}_{i2}^T \dot{\omega}_{i2} \right) + \tfrac{2}{\tau_3} \textstyle\sum_{i=1}^{N} \dot{f}_{si}^T \ddot{f}_{si} \\ &\leq \tfrac{1}{\tau_1} \textstyle\sum_{i=1}^{N} e_{i1}^T (\mathrm{He}[\bar{A} - H\bar{C}\bar{A} - J_1\bar{C}] + (\bar{D} - H\bar{C}\bar{D})(\bar{D} - H\bar{C}\bar{D})^T \\ &\quad + (\mathcal{I} - H\bar{C})(\mathcal{I} - H\bar{C})^T + \beta^2 A_0^T A_0) e_{i1} + \tfrac{1}{\tau_1} \textstyle\sum_{i=1}^{N} \left(\omega_{i1}^T \omega_{i1} + \dot{\omega}_{i2}^T \dot{\omega}_{i2} \right) \\ &\quad + \textstyle\sum_{i=1}^{N} \left((\tfrac{1}{\tau_1} - \tfrac{2\epsilon_a}{\tau_2}) \dot{f}_{ai}^T \dot{f}_{ai} + (\tfrac{1}{\tau_1} - \tfrac{2\epsilon_s}{\tau_3}) \dot{f}_{si}^T \dot{f}_{si} \right) \end{aligned} \tag{28}$$

where the nonlinear estimation error satisfies with $\|\Delta\bar{\xi}_i\|^2 \leq \beta^2 e_{i1}^T A_0^T A_0 e_{i1}$ with a Lipschitz scalar β, and $\underline{\epsilon}_a = \min_{\varrho=1,\cdots,q_1} \epsilon_a^{\varrho}, \underline{\epsilon}_s = \min_{\varrho=1,\cdots,q_2} \epsilon_s^{\varrho}$.

On the basis of the inequality constraint of P in (14), $\mathrm{He}\left[(A - BK_x)P\right] + \varphi_{\max}(\lambda_2 E_1 E_1^T + \lambda_2 I_n + P^2) + \chi_1 P < 0$ is derived with the selected scalar $\chi_1 > 0$. Applying the inequality constraint $\frac{1}{\tau_1}(\mathrm{He}[\bar{A} - H\bar{C}\bar{A} - J_1\bar{C}] + (\bar{D} - H\bar{C}\bar{D})(\bar{D} - H\bar{C}\bar{D})^T + (\mathcal{I} - H\bar{C})(\mathcal{I} - H\bar{C})^T + \beta^2 A_0^T A_0) + K^T K - \delta(E_s^T F_s^T R^T R F_s E_s + E_\omega^T E_2^T R^T R E_2 E_\omega) + \chi_2 \mathcal{I} < 0$ in (15), the derivative of the total Lyapunov function $V_1^m(t) + V_2(t)$ is derived as

$$\begin{aligned} &\dot{V}_1^m(t) + \dot{V}_2(t) < -\chi_1 \vartheta^T(t) \left(\Upsilon_{\gamma(t)} \otimes P \right) \vartheta(t) - \chi_2 e_1^T(t) e_1(t) \\ &\quad + \tfrac{1+\tau_1}{\tau_1} \omega_1^T(t) \omega_1(t) + \tfrac{1}{\tau_1} \dot{\omega}_2^T(t) \dot{\omega}_2(t) \\ &\quad + \textstyle\sum_{i=1}^{N} \left((\tfrac{1}{\tau_1} - \tfrac{2\epsilon_a}{\tau_2}) \dot{f}_{ai}^T(t) \dot{f}_{ai}(t) + (\tfrac{1}{\tau_1} - \tfrac{2\epsilon_s}{\tau_3}) \dot{f}_{si}^T(t) \dot{f}_{si}(t) \right) \\ &< -\chi_1 V_1^m(t) - \chi_2 \tau_1 V_2(t) + \tfrac{1+\tau_1}{\tau_1} \omega_1^T(t) \omega_1(t) + \tfrac{1}{\tau_1} \dot{\omega}_2^T(t) \dot{\omega}_2(t) \\ &\quad + \textstyle\sum_{i=1}^{N} \left(\tfrac{\chi_2 \tau_1 - 2\underline{\epsilon}_a}{\tau_2} + \tfrac{1}{\tau_1} \right) \dot{f}_{ai}^T(t) \dot{f}_{ai}(t) + \sum_{i=1}^{N} \left(\tfrac{\chi_2 \tau_1 - 2\underline{\epsilon}_s}{\tau_3} + \tfrac{1}{\tau_1} \right) \dot{f}_{si}^T(t) \dot{f}_{si}(t) \\ &\leq -\min\left(\chi_1, \chi_2 \tau_1\right) \left(V_1^m(t) + V_2(t) \right) + \tfrac{1+\tau_1}{\tau_1} \omega_1^T(t) \omega_1(t) + \tfrac{1}{\tau_1} \dot{\omega}_2^T(t) \dot{\omega}_2(t) \end{aligned} \tag{29}$$

where $\frac{\chi_2\tau_1}{\tau_2}+\frac{1}{\tau_1}-\frac{2\epsilon_a}{\tau_2}\leq 0$ and $\frac{\chi_2\tau_1}{\tau_3}+\frac{1}{\tau_1}-\frac{2\epsilon_s}{\tau_3}\leq 0$ are derived according to the scalar constraints (16) and (17) with the selected scalar $\chi_2>0$.

Meanwhile, under the same inequality constraint of P in another side of (14), $\mathrm{He}\left[(A-BK_x)P\right]+E_1E_1^T+I_n+\beta^2P^2-\chi_3P<0$ is given with the chosen scalar $\chi_3>0$. Under the inequality constraint $\frac{1}{\tau_1}(\mathrm{He}[\bar{A}-H\bar{C}\bar{A}-J_1\bar{C}]+(\bar{D}-H\bar{C}\bar{D})(\bar{D}-H\bar{C}\bar{D})^T+(\mathcal{I}-H\bar{C})(\mathcal{I}-H\bar{C})^T+\beta^2A_0^TA_0)+K^TK-\delta(E_s^TF_s^TR^TRF_sE_s+E_\omega^TE_2^TR^TRE_2E_\omega)-\chi_4\mathcal{I}<0$ in (15), the derivative of the total Lyapunov function $V_1^p(t)+V_2(t)$ is obtained as

$$\begin{aligned}&\dot{V}_1^p(t)+\dot{V}_2(t)<\chi_3V_1^p(t)+\chi_4\tau_1V_2(t)+\tfrac{1+\tau_1}{\tau_1}\omega_1^T(t)\omega_1(t)+\tfrac{1}{\tau_1}\dot{\omega}_2^T(t)\dot{\omega}_2(t)\\&+\textstyle\sum_{i=1}^N\left(\frac{-\chi_4\tau_1-2\epsilon_a}{\tau_2}+\frac{1}{\tau_1}\right)\dot{f}_{ai}^T(t)\dot{f}_{ai}(t)+\sum_{i=1}^N\left(\frac{-\chi_4\tau_1-2\epsilon_s}{\tau_3}+\frac{1}{\tau_1}\right)\dot{f}_{si}^T(t)\dot{f}_{si}(t)\\&\leq\max\left(\chi_3,\chi_4\tau_1\right)\left(V_1^p(t)+V_2(t)\right)+\tfrac{1+\tau_1}{\tau_1}\omega_1^T(t)\omega_1(t)+\tfrac{1}{\tau_1}\dot{\omega}_2^T(t)\dot{\omega}_2(t)\end{aligned}\tag{30}$$

where the chosen scalar $\chi_4>0$, $-\frac{\chi_4\tau_1}{\tau_2}+\frac{1}{\tau_1}-\frac{2\epsilon_a}{\tau_2}\leq 0$ and $-\frac{\chi_4\tau_1}{\tau_3}+\frac{1}{\tau_1}-\frac{2\epsilon_s}{\tau_3}\leq 0$ are also derived according to the same scalar constraints (16) and (17).

Finally, define the following total Lyapunov function $V(t,\gamma(t))$ as

$$V(t,\gamma(t))=\begin{cases}V_1^m(t)+V_2(t),\gamma(t)\in\Gamma_m\\V_1^p(t)+V_2(t),\gamma(t)\in\Gamma_p\end{cases}\tag{31}$$

Integrating both left and right sides of $\dot{V}(t,\gamma(t))$ in (31) over $t\in[t_k,t_{k+1})$,

$$V(t,\gamma(t))<\begin{cases}\xi e^{-\eta_m(t-t_k)}V(t_k,\gamma(t_k))+\frac{\xi}{\eta_m},\gamma(t)\in\Gamma_m\\\xi e^{\eta_p(t-t_k)}V(t_k,\gamma(t_k))-\frac{\xi}{\eta_p},\gamma(t)\in\Gamma_p\end{cases}\tag{32}$$

where $\eta_m=\min(\chi_1,\chi_2\tau_1),\eta_p=\max(\chi_3,\chi_4\tau_1)$ and $\xi=\frac{N}{\tau_1}((1+\tau_1)\bar{\omega}_1^2+\bar{\omega}_2^2)$ with $\bar{\omega}_1=\max\limits_{i=1,\cdots,N}\bar{\omega}_{i1}$ and $\bar{\omega}_2=\max\limits_{i=1,\cdots,N}\bar{\omega}_{i2}$.

According to the scalar condition $\max(\chi_3,\chi_4\tau_1)\geq\min(\chi_1,\chi_2\tau_1)$ in (18), for $\gamma(t)\in\Gamma=\Gamma_m\cup\Gamma_p$, it follows that

$$V(t,\gamma(t))<\xi e^{\eta_pT_p(t_k,t)-\eta_mT_m(t_k,t)}V(t_k,\gamma(t_k))\tag{33}$$

where $T_m(t_k,t)$ and $T_p(t_k,t)$ represent the total activation durations of each connectivity-maintained/-paralyzed topologies, respectively.

Since $\underline{\varphi}V_1^m(t)\leq\sum_{i=1}^Ne_{i2}^T(t)P^{-1}e_{i2}(t)\leq\overline{\varphi}V_1^m(t)$ is derived with $\underline{\varphi}=\min\limits_{i=1,\cdots,N}\varphi_{\gamma(t),i},\overline{\varphi}=\max\limits_{i=1,\cdots,N}\varphi_{\gamma(t),i}$ when $\gamma(t)\in\Gamma_m$, $V(t_k,\gamma(t_k))\leq\frac{\overline{\varphi}}{\underline{\varphi}}V(t_k^-,\gamma(t_k^-))$ is then derived at each signal switching instant $t_k,k\in\mathbb{N}$.

Undoubtedly, it is derived that

$$\begin{aligned} &V(t,\gamma(t)) < \xi e^{\eta_p T_p(t_k,t)-\eta_m T_m(t_k,t)}\tfrac{\overline{\varphi}}{\underline{\varphi}} V(t_k^-,\gamma(t_k^-)) \\ &< \xi^2 e^{\eta_p T_p(t_{k-1},t)-\eta_m T_m(t_{k-1},t)}\tfrac{\overline{\varphi}}{\underline{\varphi}} V(t_{k-1},\gamma(t_{k-1})) \\ &< \cdots < \xi^{k+1} e^{\eta_p T_p(t_0,t)-\eta_m T_m(t_0,t)}\left(\tfrac{\overline{\varphi}}{\underline{\varphi}}\right)^k V(t_0,\gamma(t_0)) \\ &= \xi e^{N_\Gamma(t_0,t)\ln\left(\frac{\xi\overline{\varphi}}{\underline{\varphi}}\right)+\eta_p T_p(t_0,t)-\eta_m T_m(t_0,t)} V(t_0,\gamma(t_0)) \end{aligned} \tag{34}$$

where the time instant k is denoted as the number of the connectivity-mixed attacks, i.e., $k = N_\Gamma(t_0,t)$.

Since the connectivity-mixed attack frequency $\mathcal{F}_\Gamma(t_0,t)$ (19) is satisfied, $N_\Gamma(t_0,t)\ln(\frac{\xi\overline{\varphi}}{\underline{\varphi}}) \le (\rho^\star-\rho_\Gamma)(t-t_0)$ is then derived. Furthermore, $\eta_p T_p(t_0,t) - \eta_m T_m(t_0,t) \le -\rho^\star(t-t_0)$ is derived on the basis of the scalar inequalities (20) of the connectivity-maintained/-paralyzed attack activation rates, i.e., $\mathcal{R}_{\Gamma_m}(t_0,t) \ge \frac{\eta_p+\rho^\star}{\eta_m+\eta_p}$ and $\mathcal{R}_{\Gamma_p}(t_0,t) \le \frac{\eta_m-\rho^\star}{\eta_m+\eta_p}$. Then, it is derived that $N_\Gamma(t_0,t)\ln\left(\frac{\xi\overline{\varphi}}{\underline{\varphi}}\right) + \eta_p T_p(t_0,t) - \eta_m T_m(t_0,t) \le -\rho_\Gamma(t-t_0)$, and it follows that

$$V(t,\gamma(t)) < \xi e^{-\rho_\Gamma(t-t_0)} V(t_0,\gamma(t_0)) \tag{35}$$

According to the definition of $V(t,\gamma(t)), \gamma(t) \in \Gamma$ in (31), the total Lyapunov function $V(t_0,\gamma(t_0))$ with the initial instant t_0 is given as

$$\begin{aligned} &V(t_0,\gamma(t_0)) \le \max\left(\lambda_{\max}(\varphi_{\gamma(t),i}^{-1}P^{-1}), \lambda_{\max}(P^{-1})\right)\textstyle\sum_{i=1}^N \|e_{i2}(t_0)\|^2 \\ &+\frac{\max\limits_{i=1,\cdots,N}\left(\frac{1}{\tau_1}\|e_{i1}(t_0)\|^2+\frac{1}{\tau_2}\|\dot{f}_{ai}(t_0)\|^2+\frac{1}{\tau_3}\|\dot{f}_{si}(t_0)\|^2\right)}{\min\limits_{i=1,\cdots,N}\|e_{i2}(t_0)\|^2}\textstyle\sum_{i=1}^N \|e_{i2}(t_0)\|^2 \end{aligned} \tag{36}$$

Introduce the new parameter $\Lambda_\Gamma = \max(\lambda_{\max}(\varphi_{\gamma(t),i}^{-1}P^{-1}), \lambda_{\max}(P^{-1})) + \sigma_\Gamma$ for $\gamma(t) \in \Gamma_m$ with the appropriate positive scalar σ_Γ, it follows that

$$\begin{aligned} &\min\left(\lambda_{\min}(\varphi_{\gamma(t),i}^{-1}P^{-1}), \lambda_{\min}(P^{-1})\right)\textstyle\sum_{i=1}^N \|e_{i2}(t)\|^2 \le V(t,\gamma(t)) \\ &< \xi e^{-\rho_\Gamma(t-t_0)} V(t_0,\gamma(t_0)) \le \xi\Lambda_\Gamma e^{-\rho_\Gamma(t-t_0)}\textstyle\sum_{i=1}^N \|e_{i2}(t_0)\|^2 \end{aligned} \tag{37}$$

and the leader-following consensus error finally yields that

$$\begin{aligned} &\|x_i(t)-x_0(t)\|^2 = \|e_{i2}(t)\|^2 \le \frac{\xi\Lambda_\Gamma e^{-\rho_\Gamma(t-t_0)}\|e_{i2}(t_0)\|^2}{\min\left(\lambda_{\min}(\varphi_{\gamma(t),i}^{-1}P^{-1}), \lambda_{\min}(P^{-1})\right)} \\ &= \mu_\Gamma e^{-\rho_\Gamma(t-t_0)}\|e_{i2}(t_0)\|^2 = \mu_\Gamma e^{-\rho_\Gamma(t-t_0)}\|x_i(t_0)-x_0(t_0)\|^2 \end{aligned} \tag{38}$$

with

$$\mu_{\Gamma}=\frac{N((1+\tau_1)\bar{\omega}_1^2+\bar{\omega}_2^2)\Big(\max\Big(\lambda_{\max}(\varphi_{\gamma(t),i}^{-1}P^{-1}),\lambda_{\max}(P^{-1})\Big)+\sigma_{\Gamma}\Big)}{\tau_1\min\Big(\lambda_{\min}(\varphi_{\gamma(t),i}^{-1}P^{-1}),\lambda_{\min}(P^{-1})\Big)} \tag{39}$$

Remark 3: The bi-linear property of the nonlinear matrix inequality (15) causes the inequality to be complicated and tedious to obtain a suitable solution, thus using Schur's Lemma and parametric matrix decomposability H and J_1, the inequality (15) can be derived solvability from the following multi-dimensional and easily constructed linear matrix inequality.

$$\begin{bmatrix}
\Omega_{11} & \Omega_{12} & \Omega_{13} & \Omega_{14} & I_n-H_1C & \mathbf{0}_{n\times q_1} & -H_1F_s & -H_1E_2\\
\star & \Omega_{22} & \Omega_{23} & \Omega_{24} & -H_2C & I_{q_1} & -H_2F_s & -H_2E_2\\
\star & \star & \Omega_{33} & \Omega_{34} & -H_3C & \mathbf{0}_{q_2\times q_1} & I_{q_2}-H_3F_s & -H_3E_2\\
\star & \star & \star & \Omega_{44} & -H_4C & \mathbf{0}_{s_2\times q_1} & -H_4F_s & I_{s_2}-H_4E_2\\
\star & \star & \star & \star & \Omega_{55} & \mathbf{0}_{n\times q_1} & \mathbf{0}_{n\times q_2} & \mathbf{0}_{n\times s_2}\\
\star & \star & \star & \star & \star & -\frac{\tau_1}{2}I_{q_1} & \mathbf{0}_{q_1\times q_2} & \mathbf{0}_{q_1\times s_2}\\
\star & \star & \star & \star & \star & \star & -\frac{\tau_1}{2}I_{q_2} & \mathbf{0}_{q_2\times s_2}\\
\star & \star & \star & \star & \star & \star & \star & -\frac{\tau_1}{2}I_{s_2}
\end{bmatrix}<0 \tag{40}$$

where $\Omega_{11}=\frac{1}{\tau_1}\mathrm{He}[A-H_1CA-J_{11}C]+K_x^TK_x+(\frac{\beta^2}{\tau_1}+\chi_2)I_n,\Omega_{12}=\frac{1}{\tau_1}(F_a-H_1CF_a-A^TC^TH_2^T-C^TJ_{12}^T)+K_x^TK_a,\Omega_{13}=-\frac{1}{\tau_1}(J_{11}F_s+A^TC^TH_3^T+C^TJ_{13}^T),\Omega_{14}=-\frac{1}{\tau_1}(J_{11}E_2+A^TC^TH_4^T+C^TJ_{14}^T),\Omega_{22}=-\frac{1}{\tau_1}\mathrm{He}[H_2CF_a]+K_a^TK_a+\chi_2I_{q_1},\Omega_{23}=-\frac{1}{\tau_1}(J_{12}F_s+F_a^TC^TH_3^T),\Omega_{24}=-\frac{1}{\tau_1}(J_{12}E_2+F_a^TC^TH_4^T),\Omega_{33}=-\frac{1}{\tau_1}\mathrm{He}[J_{13}F_s]-\sigma F_s^TR^TRF_s+\chi_2I_{q_2},\Omega_{34}=-\frac{1}{\tau_1}(J_{13}E_2+F_s^TJ_{14}^T),\Omega_{44}=\chi_2I_{s_2}-\frac{1}{\tau_1}\mathrm{He}[J_{14}E_2]-\sigma E_2^TR^TRE_2,\Omega_{55}=-\tau_1(E_1E_1^T+I_n)$ with $H=[H_1^T\ H_2^T\ H_3^T\ H_4^T]^T$ and $J_1=[J_{11}^T\ J_{12}^T\ J_{13}^T\ J_{14}^T]^T$.

Remark 4: (i) In contrast to traditional auxiliary strategies for state observer [11] or disturbance observer [14], i.e., fuzzy logic approximation [10], adaptive compensation [16] and neural networks evaluation [12], [14], it is interestingly found that a less conservative calculation of gain matrices H and J_1 in augmented estimation-based observer mechanism applies the model normalization and decoupling without any challenges to equality solvability in our previous study [35], which simplifies the computational decentralized information interaction at the observer layer. (ii) The novel distributed fault-tolerant consensus control module is devised for achieving node-to-node consensus by exploiting the set of available output collections from the neighboring followers as well as local sensor fault/output channel noise estimations and augmented state observation. To eliminate the adverse effects of simul-

taneous actuator/sensor faults and channel noises in the physical layer and connectivity-mixed attacks in the cyber layer on the augmented estimation error dynamics (9) and leader-following consensus error dynamics (12), the ADT index [28], [33] is avoided with the aid of dual attack frequency and activation rates (19) and (20). In addition, multi-step computation of parameters in Theorem 1 with recursive linear matrix inequality (40) is derived for the quantitative relationship among the exponential leader-following consensus performance, decay rate/amplitude bounds, and multi-agent numbers.

4. Simulation Results

In this section, two simulation cases are put forward to illustrate the effectiveness and validation of comparative analysis (ADT-based fault-tolerant consensus control algorithm [35] and the proposed dual attack indicators-based fault-tolerant consensus algorithm), i.e., case 1 with multi-machine power systems and case 2 with multi-aircraft systems.

4.1. Case 1: multi-machine power systems

The multi-machine power system matrices describe the dynamic behavior of each machine as follows [15]

$$A=\begin{bmatrix} 0 & 1 & 0 & 0 \\ 0 & -0.2941 & 30.7999 & 0 \\ 0 & 0 & -2.8571 & 2.8571 \\ 0 & 0.6366 & 0 & -10 \end{bmatrix}, B=\begin{bmatrix} 0 \\ 0 \\ 0 \\ 10 \end{bmatrix}, C=\begin{bmatrix} 1 & 0 & 0 & 0 \\ 0 & 1 & 0 & 0 \end{bmatrix} \tag{41}$$

The state vector of each machine in multi-machine power systems is denoted as $x_i(t)=[\Delta\sigma_i^T\ \Delta\omega_i^T\ \Delta P_{mi}^T\ \Delta X_{ei}^T]^T, i=0,\cdots,6$, where $\Delta\sigma_i$ is the rotor angle deviation, $\Delta\omega_i$ is the speed deviation, ΔP_{mi} is the mechanical power deviation, and ΔX_{ei} is the steam valve aperture deviation. Furthermore, denote the leader-following consensus error as $e_{i2}=[e_{i2}^{\sigma}\ e_{i2}^{\omega}\ e_{i2}^{P}\ e_{i2}^{X}]^T, i=1,\cdots,6$.

The noise distribution matrices are set as $E_1=[0.8\ 0.9\ 1\ 0]^T$ and $E_2=[0.75\ 0.95]^T$, the specific input and output channel noises with machine numbers $N=6$ are settled as $\omega_{i1}(t)=0.9\sin(0.8t), \omega_{i2}(t)=0.5\sin(1.5t)$. The Lipschitz nonlinear interconnection is denoted as $\xi(x_i(t),t)=\sum_{j=1}^{6}\sin(\Delta\sigma_i-\Delta\sigma_j)$. The selected physical fault distribution matrices $F_a=[0\ 0\ 0\ 1.5]^T, F_s=[1.5\ \ 0.8]^T$ with the lower and upper boundaries of the decay rates $\underline{\epsilon}_{a(s)}=0.005, \overline{\epsilon}_{a(s)}=0.1$ and the specific unified incipient-/abrupt-type actuator and

sensor faults $f_{ai}(t), f_{si}(t)$ in the presence of steam valve aperture actuator faults and sensor faults in the rotor angle and relative speed measuring channels are set as

$$\begin{aligned}
&\text{Machine 1, Machine 2 : normal/healthy operation}\\
&\text{Machine 3 :} f_{a3}(t) = \begin{cases} 1-e^{-0.2t}), t \leq 70\text{s} \\ 1.2(1-e^{-0.6t}), \text{otherwise} \end{cases}\\
&\text{Machine 4 :} f_{s4}(t) = \begin{cases} 0, t \leq 40\text{s} \\ 1-e^{-0.5t}, \text{otherwise} \end{cases}\\
&\text{Machine 5 :} f_{s5}(t) = \begin{cases} 0.07(1-e^{-0.06t}), t \leq 90\text{s} \\ 0.05(1-e^{-0.06t}), \text{otherwise} \end{cases}\\
&\text{Machine 6 :} f_{a6}(t) = \begin{cases} 0.03(1-e^{-0.05t}), t \leq 10\text{s} \\ 0.07(1-e^{-0.05t}), \text{otherwise} \end{cases}
\end{aligned} \tag{42}$$

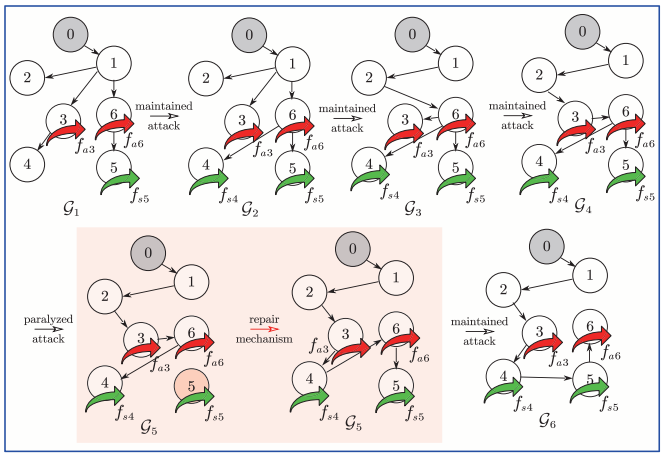

Figure 2: Switching of connectivity-maintained and connectivity-paralyzed topologies under connectivity-mixed attacks.

The switching connectivity-maintained and connectivity-paralyzed topologies under connectivity-mixed attacks are shown in Figure 2, in which $\mathcal{G}_1$ denotes the initial graph during 0s-30s, $\mathcal{G}_2$-$\mathcal{G}_4$ denote the connectivity-maintained topologies (30s-50s,50s-80s,80s-100s), $\mathcal{G}_5$ represents the connectivity-paralyzed topology that can recover connected through the repair mechanism within 100s-110s, and finally $\mathcal{G}_6$ denotes the maintained connectivity during 110s-120s. Furthermore, the positive simulation parameters in Theorem 1 are

calculated and preset as $\chi_1 = 0.55, \chi_2 = 0.0036, \chi_3 = 0.8, \chi_4 = 0.064, \tau_1 = 12.5, \tau_2 = 0.63, \tau_3 = 0.5, \delta_0 = 1.25$ and $\sigma_\Gamma = 0.005$.

In the presence of unified actuator/sensor faults and channel noises in the physical layer and connectivity-mixed attacks in the cyber layer, the rotor angle, speed, mechanical power, and steam valve aperture deviation errors in Figure 3-Figure 6 all show dramatic fluctuations at the moment of fault action and topology switching due to attacks. However, the fault-tolerant consensus control algorithm based on the distributed anti-attack strategy still achieves efficient and fast convergence. The following three points are of concern. 1) The abrupt actuator/sensor faults occurring at 40s and 70s have a greater impact on the error tracking signal, i.e., the abrupt-type faults with larger amplitude and faster rate are prone to spikes at each fault occurring instant. The unified abrupt-/incipient-type faults occurring at 10s and 90s are compressed to non-significance along with channel noises due to the strong robustness of the fault tolerant consensus compensation mechanism. 2) The amplitude of the oscillations at the moment of topology switching is incremental, which indicates that even if the topology is only a single link change, the system effect is cumulative for each topology switching. The existence of an anti-attack algorithm only guarantees the effectiveness of this considered attack, and over time the limits of the anti-attack resistance must be exceeded (attack frequency, attack activation rate indicators are no longer satisfied). 3) The proposed dual attack indicators-based fault-tolerant consensus algorithm has faster convergence and smaller oscillations than the ADT-based fault-tolerant consensus control algorithm [35], and is more robust to $\sin, \cos$-type noises and no longer exhibits periodic reciprocity. Furthermore, Figure 7 illustrates the state estimation errors in multi-power machine systems under connectivity-mixed attacks and actuator/sensor faults.

4.2. Case 2: multi-aircraft systems

The following system matrices describe the dynamic behavior of each aircraft as follows [9]

$$A = \begin{bmatrix} -2.98 & 0.93 & 0 & -0.034 \\ -0.99 & -0.21 & 0.035 & -0.0011 \\ 0 & 0 & -2 & 1 \\ 0.39 & -5.555 & 0 & -1.89 \end{bmatrix}, B = \begin{bmatrix} -0.032 & 0.5 & 1.55 \\ 0 & 0 & 0 \\ 0 & 0 & 0 \\ -1.6 & 1.8 & -2 \end{bmatrix} \tag{43}$$

The state of each aircraft in multi-aircraft systems is denoted as $x_i(t) = [x_{i1}^T \; x_{i2}^T \; x_{i3}^T \; x_{i4}^T]^T, i = 0, \cdots, 6$. The leader-following consensus error is denoted

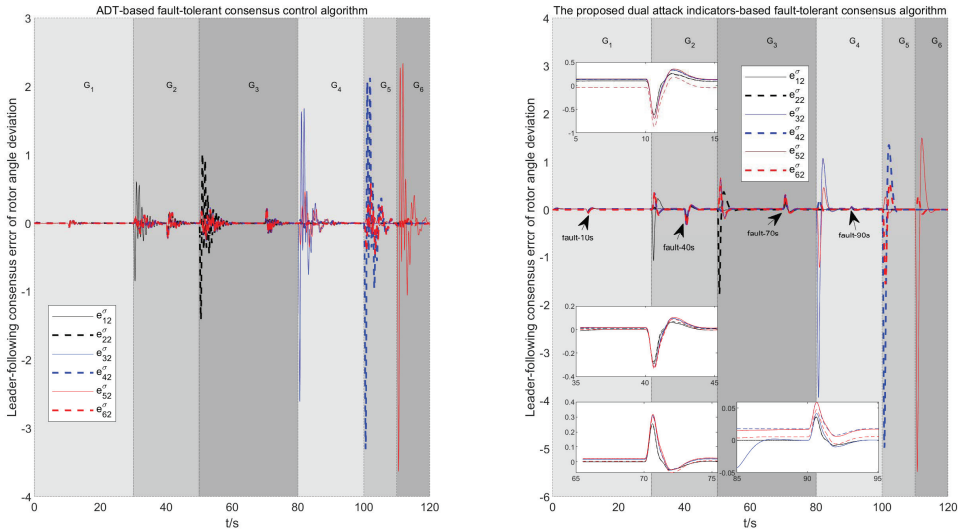

Figure 3: Comparison of rotor angle deviation errors through the proposed dual attack indicators-based and ADT-based [35] fault-tolerant consensus control algorithms.

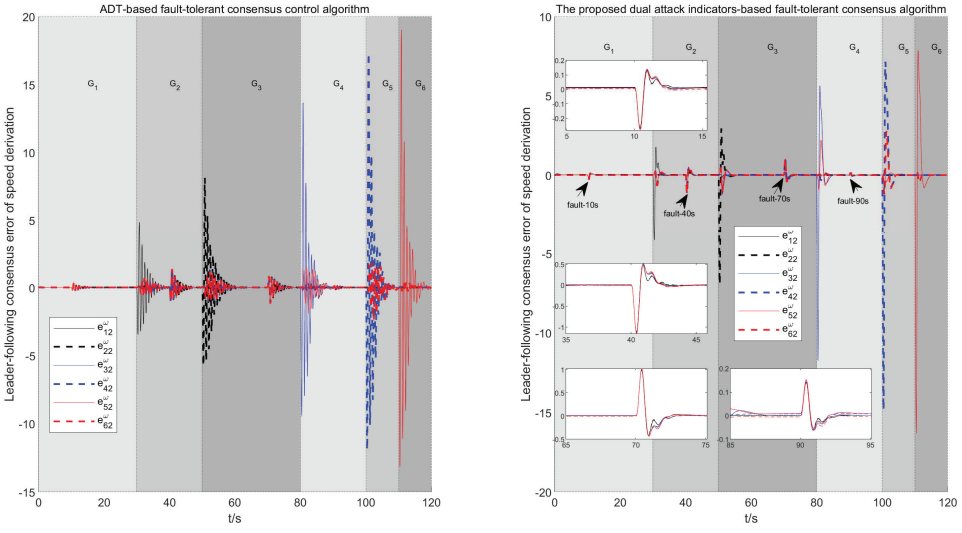

Figure 4: Comparison of speed deviation errors through the proposed dual attack indicators-based and ADT-based [35] fault-tolerant consensus control algorithms.

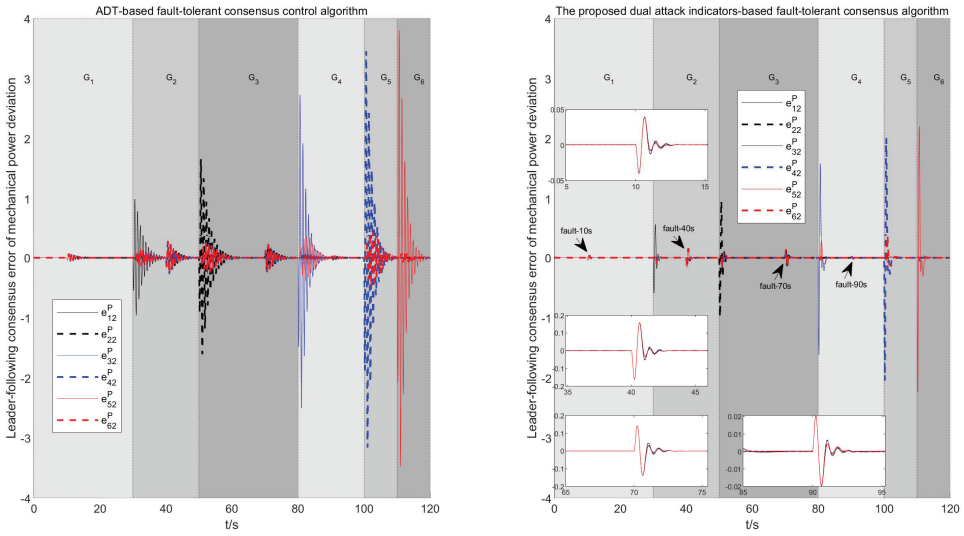

Figure 5: Comparison of mechanical power deviation errors through the proposed dual attack indicators-based and ADT-based [35] fault-tolerant consensus control algorithms.

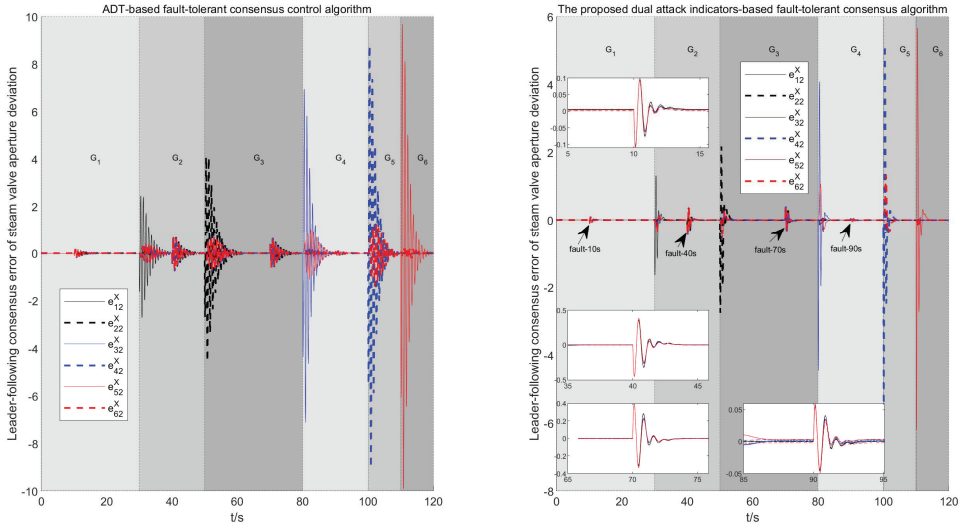

Figure 6: Comparison of steam valve aperture deviation errors through the proposed dual attack indicators-based and ADT-based [35] fault-tolerant consensus control algorithms.

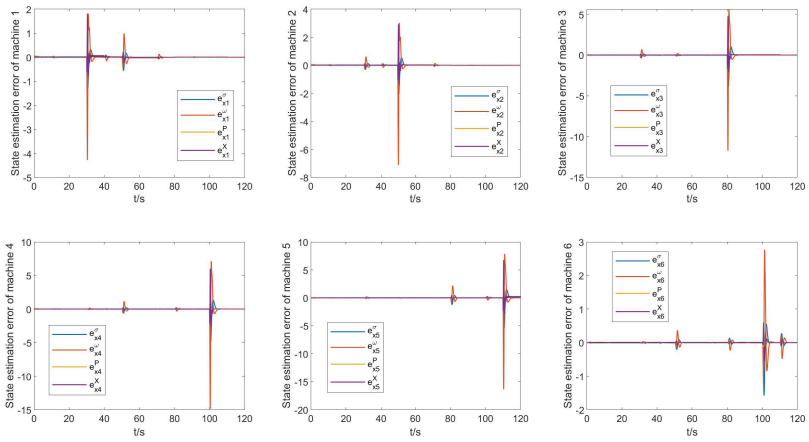

Figure 7: State estimation errors in multi-power machine systems under connectivity-mixed attacks and actuator/sensor faults.

as $e_{i2} = [e_{i2}^1\ e_{i2}^2\ e_{i2}^3\ e_{i2}^4]^T, i = 1, \cdots, 6$. The output channel matrix C is preset as mentioned in Case 1. The noise distribution matrices are set as $E_1 = [1.2\ 0.5\ 0\ 1.5]^T, E_2 = [1.25\ 0.85]^T$, the nonlinear function and channel noises are selected as $\xi(x_i(t), t) = [0.67\sin(x_{i1}(t))\ \ 0\ \ 0.35\cos(x_{i3}(t))\ \ 0]^T, \omega_{i1}(t) = 0.5(1 + 0.5\sin(0.2t)), \omega_{i2}(t) = 1.2\sin(0.5t)$. The physical fault distribution matrices $F_a = [0.8\ \ 0\ \ 0\ \ 1.3]^T, F_s = [-0.85\ \ 1.3]^T$ and the specific unified incipient-/abrupt-type actuator/sensor faults $f_{ai}(t), f_{si}(t)$ are set as

$$\begin{aligned}
&\text{Aircrafts } 1, 2, 6 : \text{fault free, Aircrafts } 3, 4, 5 : \text{fault} \\
&f_{s3}(t) = 0.7(1 - e^{-0.06t}), [90\text{s}, 120\text{s}], f_{s4}(t) = 1 - e^{-0.05t}, [70\text{s}, 120\text{s}] \\
&f_{a5}(t) = \begin{cases} 1 - e^{-0.2t}), [10\text{s}, 40\text{s}) \\ 1.2(1 - e^{-0.6t}), [40\text{s}, 70\text{s}) \\ -(1 - e^{-0.6t}), [70\text{s}, 90\text{s}) \\ 1.2(1 - e^{-0.2t}), [90\text{s}, 120\text{s}] \end{cases}
\end{aligned} \tag{44}$$

The state-estimation gain is derived as $K_x = [-1.0315\ \ -3.0695\ 1.4691\ \ -1.7447]$ under the considered cyber-physical threats. i.e., the fault occurring time instants $10\text{s}, 40\text{s}, 70\text{s}, 90\text{s}$ and the attack occurring time instants $30\text{s}, 50\text{s}, 80\text{s}, 100\text{s}, 110\text{s}$.

Figure 8 illustrates the four-channel state consensus errors of multi-aircraft systems under the influence of connectivity-mixed attacks, uniform abrupt-/incipient-type actuator/sensor faults and channel noises. Actuator/sensor faults occurring at 10s, 40s, 70s and 90s have a greater fluctuation on aircrafts 3, 4 and 5, while switching moments at 30s, 50s, 80s, 100s and 110s

have a greater effect on aircrafts 1-5 with increasing cumulative fluctuations. Figure 9 depicts the state estimation errors of multi-aircraft systems under hostile connectivity-mixed attacks and unified actuator/sensor faults. At the moment of network attack topology switching, which has a large influence on the dynamical system, the fault-tolerant consensus control algorithm based on the distributed anti-attack mechanism achieves efficient and fast convergence despite the presence of oscillatory reciprocity.

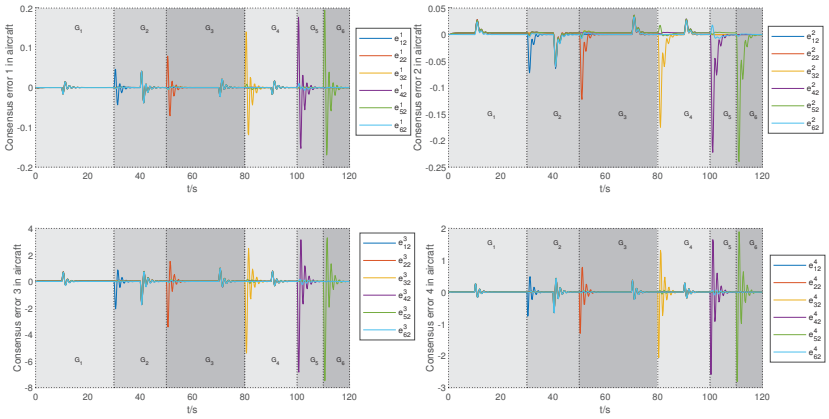

Figure 8: State consensus errors in four channels of multi-aircraft systems under connectivity-mixed attacks and actuator/sensor faults.

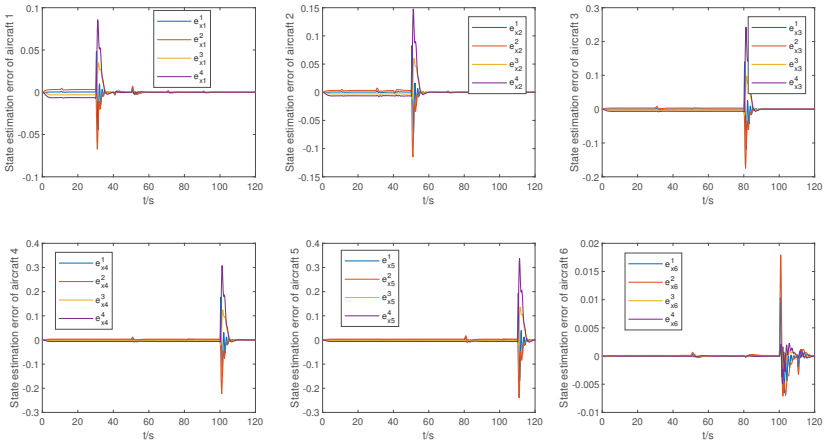

Figure 9: State estimation errors in multi-aircraft systems under connectivity-mixed attacks and actuator/sensor faults.

5. Conclusions

An integrated co-design of normalization/estimation-based observer design and distributed anti-attack fault-tolerant consensus control method is developed in this study to guarantee the exponential leader-following consensus of nonlinear MASs under the influence of incipient-/abrupt-type actuator/sensor faults and channel noises in the physical layer and hostile connectivity-mixed attacks in the cyber layer. The tolerance to faults, resiliency against attacks, and robustness to noises are considered through the safety/security analysis of leader-following consensus restoration proof using rigorous Lyapunov analysis. Sufficient criteria are proposed to bridge the quantitative relationship between the prescribed anti-attack fault-tolerant consensus performance and dual attack frequency and activation rate indicators. Two simulation studies, including multi-helicopter and multi-machine power systems, with various anti-attack fault-tolerant configurations demonstrate the efficiency of the algorithm. Future investigations of more general nonlinear continuous and discrete MASs towards novel anti-attack and tolerance capabilities to address physical faults, interruptive attacks, and even multiple and replay attacks are highlighted.

References

[1] Gao C, He X, Dong H, Liu H, Lyu G. A survey on fault-tolerant consensus control of multi-agent systems: trends, methodologies and prospects. International Journal of Systems Science 2022;doi:10.1080/00207721.2022.2056772.

[2] Shahab MA, Mozafari B, Soleymani S, Dehkordi NM, Shourkaei HM, Guerrero JM. Distributed consensus-based fault tolerant control of islanded microgrids. IEEE Transactions on Smart Grid 2020;11(1):37–47. doi:10.1109/TSG.2019.2916727.

[3] Lin X, Tian W, Zhang W, Zeng J, Zhang C. The leaderless multi-AUV system fault-tolerant consensus strategy under heterogeneous communication topology. Ocean Engineering 2021;237. doi:10.1016/j.oceaneng.2021.109594.

[4] Hashemi E, Pirani M, Khajepour A, Fidan B, Chen Sk, Litkouhi B. Fault tolerant consensus for vehicle state estimation: a cyber-physical ap-

proach. IEEE Transactions on Industrial Informatics 2019;15(9):5129–5138. doi:10.1109/tii.2019.2898170.

[5] Yu Z, Qu Y, Zhang Y. Distributed fault-tolerant cooperative control for multi-UAVs under actuator fault and input saturation. IEEE Transactions on Control Systems Technology 2019;27(6):2417–2429. doi:10.1109/TCST.2018.2868038.

[6] Ye D, Chen MM, Yang HJ. Distributed adaptive event-triggered fault-tolerant consensus of multiagent systems with general linear dynamics. IEEE Transactions on Cybernetics 2019;49(3):757–767. doi:10.1109/TCYB.2017.2782731.

[7] Gong P, Lan W, Han QL. Robust adaptive fault-tolerant consensus control for uncertain nonlinear fractional-order multi-agent systems with directed topologies. Automatica 2020;117. doi:10.1016/j.automatica.2020.109011.

[8] Li K, Li Y. Fuzzy adaptive optimal consensus fault-tolerant control for stochastic nonlinear multi-agent systems. IEEE Transactions on Fuzzy Systems 2021;doi:10.1109/tfuzz.2021.3094716.

[9] Sader M, Chen Z, Liu Z, Deng C. Distributed robust fault-tolerant consensus control for a class of nonlinear multi-agent systems with intermittent communications. Applied Mathematics and Computation 2021;403. doi:10.1016/j.amc.2021.126166.

[10] Zou W, Ahn CK, Xiang Z. Fuzzy-approximation-based distributed fault-tolerant consensus for heterogeneous switched nonlinear multiagent systems. IEEE Transactions on Fuzzy Systems 2021;29(10):2916–2925. doi:10.1109/TFUZZ.2020.3009730.

[11] Cai Y, Zhang H, Li W, Mu Y, He Q. Distributed bipartite adaptive event-triggered fault-tolerant consensus tracking for linear multiagent systems under actuator faults. IEEE Transactions on Cybernetics 2021;doi:10.1109/TCYB.2021.3069955.

[12] Wu W, Li Y, Tong S. Neural network output-feedback consensus fault-tolerant control for nonlinear mltiagent systems with intermittent actuator faults. IEEE Transactions on Neural Networks and Learning Systems 2021;doi:10.1109/TNNLS.2021.3117364.

[13] Yu Y, Peng S, Dong X, Li Q, Ren Z. UIF-based cooperative tracking method for multi-agent systems with sensor faults. Science China Information Sciences 2019;62(1):1–14. doi:10.1007/s11432-018-9581-y.

[14] Cao L, Li H, Dong G, Lu R. Event-triggered control for multiagent systems with sensor faults and input saturation. IEEE Transactions on Systems, Man, and Cybernetics: Systems 2021;51(6):3855–3866. doi:10.1109/TSMC.2019.2938216.

[15] Liu C, Jiang B, Patton RJ, Zhang K. Hierarchical-structure-based fault estimation and fault-tolerant control for multiagent systems. IEEE Transactions on Control of Network Systems 2018;6(2):586–597.

[16] Chen C, Lewis FL, Xie S, Modares H, Liu Z, Zuo S, Davoudi A. Resilient adaptive and H_∞ controls of multi-agent systems under sensor and actuator faults. Automatica 2019;102:19–26. doi:10.1016/J.AUTOMATICA.2018.12.024.

[17] Huang C, Xie S, Liu Z, Chen CP, Zhang Y. Adaptive inverse optimal consensus control for uncertain high-order multiagent systems with actuator and sensor failures. Information Sciences 2022;605:119–135. doi:https://doi.org/10.1016/j.ins.2022.05.021.

[18] Wu Y, Liu J, Wang Z, Ju Z. Distributed resilient tracking of multiagent systems under actuator and sensor faults. IEEE Transactions on Cybernetics 2021;doi:10.1109/TCYB.2021.3132380.

[19] Wang Z, Sun H, Zhang H, Liu X. Bounded consensus control for stochastic multi-agent systems with additive noises. Neurocomputing 2020;408:72–79. doi:https://doi.org/10.1016/j.neucom.2019.11.027.

[20] Hu J, Wu Y, Li T, Ghosh BK. Consensus control of general linear multiagent systems with antagonistic interactions and communication noises. IEEE Transactions on Automatic Control 2019;64(5):2122–2127. doi:10.1109/TAC.2018.2872197.

[21] Zou W, Xiang Z, Ahn CK. Mean square leader-following consensus of second-order nonlinear multiagent systems with noises and unmodeled dynamics. IEEE Transactions on Systems, Man, and Cybernetics: Systems 2019;49(12):2478–2486. doi:10.1109/TSMC.2018.2862140.

[22] Ishii H, Wang Y, Feng S. An overview on multi-agent consensus under adversarial attacks. Annual Reviews in Control 2022;doi:https://doi.org/10.1016/j.arcontrol.2022.01.004.

[23] Meng M, Xiao G, Li B. Adaptive consensus for heterogeneous multi-agent systems under sensor and actuator attacks. Automatica 2020;122. doi:https://doi.org/10.1016/j.automatica.2020.109242.

[24] He W, Gao X, Zhong W, Qian F. Secure impulsive synchronization control of multi-agent systems under deception attacks. Information Sciences 2018;459:354–368. doi:10.1016/j.ins.2018.04.020.

[25] Tahoun A, Arafa M. Cooperative control for cyber–physical multi-agent networked control systems with unknown false data-injection and replay cyber-attacks. ISA Transactions 2021;110:1–14. doi:10.1016/j.isatra.2020.10.002.

[26] Feng Z, Hu G. Secure cooperative event-triggered control of linear multiagent systems under DoS attacks. IEEE Transactions on Control Systems Technology 2019;28(3):741–752. doi:10.1109/TCST.2019.2892032.

[27] Jin X, Lü S, Deng C, Chadli M. Distributed adaptive security consensus control for a class of multi-agent systems under network decay and intermittent attacks. Information Sciences 2021;547:88–102. doi:https://doi.org/10.1016/j.ins.2020.08.013.

[28] Wen G, Wang P, Huang T, Lü J, Zhang F. Distributed consensus of layered multi-agent systems subject to attacks on edges. IEEE Transactions on Circuits and Systems I: Regular Papers 2020;67(9):3152–3162. doi:10.1109/TCSI.2020.2986953.

[29] Zhang D, Feng G, Shi Y, Srinivasan D. Physical safety and cyber security analysis of multi-agent systems: a survey of recent advances. IEEE/CAA Journal of Automatica Sinica 2021;8(2):319–333. doi:10.1109/JAS.2021.1003820.

[30] Li Y, Fang H, Chen J. Anomaly detection and identification for multiagent systems subjected to physical faults and cyberattacks. IEEE Transactions on Industrial Electronics 2020;67(11):9724–9733. doi:10.1109/TIE.2019.2952802.

[31] Zhao L, Yang GH. Cooperative adaptive fault-tolerant control for multi-agent systems with deception attacks. Journal of the Franklin Institute 2020;357(6):3419–3433. doi:10.1016/j.jfranklin.2019.12.032.

[32] Guo XG, Liu PM, Wang JL, Ahn CK. Event-triggered adaptive fault-tolerant pinning control for cluster consensus of heterogeneous nonlinear multi-agent systems under aperiodic DoS attacks. IEEE Transactions on Network Science and Engineering 2021;8(2):1941–1956. doi:10.1109/TNSE.2021.3077766.

[33] Zhao L, Yang GH. Adaptive fault-tolerant control for nonlinear multi-agent systems with DoS attacks. Information Sciences 2020;526:39–53. doi:10.1016/j.ins.2020.03.083.

[34] Zhang Z, Dong J. Fault-tolerant containment control for IT2 fuzzy networked multiagent systems against denial-of-service attacks and actuator faults. IEEE Transactions on Systems, Man, and Cybernetics: Systems 2022;52(4):2213–2224. doi:10.1109/TSMC.2020.3048999.

[35] Liu C, Jiang B, Zhang K, Patton RJ. Distributed fault-tolerant consensus tracking control of multi-agent systems under fixed and switching topologies. IEEE Transactions on Circuits and Systems I: Regular Papers 2021;68(4):1646–1658. doi:10.1109/TCSI.2021.3049347.

[36] Shen H, Wang Y, Xia J, Park JH, Wang Z. Fault-tolerant leader-following consensus for multi-agent systems subject to semi-markov switching topologies: an event-triggered control scheme. Nonlinear Analysis: Hybrid Systems 2019;34:92–107. doi:10.1016/j.nahs.2019.05.003.